2017

Behavior of Different Sizes of Strontium Titanate Substrates in Electrochemical Modifications

Shuxin Luo
Eastern Illinois University

The Graduate School
EASTERN ILLINOIS UNIVERSITY

Thesis Maintenance and Reproduction Certificate

FOR: Graduate Candidates Completing Theses in Partial Fulfillment of the Degree
Graduate Faculty Advisors Directing the Theses

RE: Preservation, Reproduction, and Distribution of Thesis Research

---

Preserving, reproducing, and distributing thesis research is an important part of Booth Library's responsibility to provide access to scholarship. In order to further this goal, Booth Library makes all graduate theses completed as part of a degree program at Eastern Illinois University available for personal study, research, and other not-for-profit educational purposes. Under 17 U.S.C. § 108, the library may reproduce and distribute a copy without infringing on copyright; however, professional courtesy dictates that permission be requested from the author before doing so.

Your signatures affirm the following:

- The graduate candidate is the author of this thesis.
- The graduate candidate retains the copyright and intellectual property rights associated with the original research, creative activity, and intellectual or artistic content of the thesis.
- The graduate candidate certifies her/his compliance with federal copyright law (Title 17 of the U. S. Code) and her/his right to authorize reproduction and distribution of all copyrighted materials included in this thesis.
- The graduate candidate in consultation with the faculty advisor grants Booth Library the non-exclusive, perpetual right to make copies of the thesis freely and publicly available without restriction, by means of any current or successive technology, including by not limited to photocopying, microfilm, digitization, or internet.
- The graduate candidate acknowledges that by depositing her/his thesis with Booth Library, her/his work is available for viewing by the public and may be borrowed through the library's circulation and interlibrary loan departments, or accessed electronically.
- The graduate candidate waives the confidentiality provisions of the Family Educational Rights and Privacy Act (FERPA) (20 U. S. C. § 1232g; 34 CFR Part 99) with respect to the contents of the thesis and with respect to information concerning authorship of the thesis, including name and status as a student at Eastern Illinois University.

I have conferred with my graduate faculty advisor. My signature below indicates that I have read and agree with the above statements, and hereby give my permission to allow Booth Library to reproduce and distribute my thesis. My adviser's signature indicates concurrence to reproduce and distribute the thesis.

Graduate Candidate Signature _____ Faculty Adviser Signature _____

Printed Name _____ Printed Name _____

Ms. in Chemistry
Graduate Degree Program

05/31/2017
Date

Please submit in duplicate.

Behavior of Different Sizes of Strontium Titanate Substrates in Electrochemical Modifications

(TITLE)

BY

Shuxin Luo

THESIS

SUBMITTED IN PARTIAL FULFILLMENT OF THE REQUIREMENTS
FOR THE DEGREE OF

Master of Science in Chemistry

IN THE GRADUATE SCHOOL, EASTERN ILLINOIS UNIVERSITY
CHARLESTON, ILLINOIS

2017

YEAR

I HEREBY RECOMMEND THAT THIS THESIS BE ACCEPTED AS FULFILLING
THIS PART OF THE GRADUATE DEGREE CITED ABOVE

05/30/17			
THESIS COMMITTEE CHAIR	DATE	DEPARTMENT/SCHOOL CHAIR OR CHAIR'S DESIGNEE	DATE
5/19/17		05/30/17	
THESIS COMMITTEE MEMBER	DATE	THESIS COMMITTEE MEMBER	DATE
5/19/17		5/19/17	
THESIS COMMITTEE MEMBER	DATE	THESIS COMMITTEE MEMBER	DATE

Behavior of Different Sizes of Strontium Titanate Substrates in Electrochemical Modification

Shuxin Luo

Research Advisor: Dr. Svetlana Mitrovski

Eastern Illinois University

The Department of Chemistry

Abstract

In our previous atomic force microscopy (AFM) studies of 5 mm × 5 mm single crystal $SrTiO_3$ (STO(100)) substrates, rutile TiO_2 crystals were found on the substrates surfaces after electrochemical modification. These crystals were found mainly in the area of contact between the substrate and the gold-coated alligator clip that was not supposed to be immersed into the electrolyte and that served as a connection between the STO working electrode and the potentiostat circuit. The size and density of the crystals were found to depend on electrochemical potential, its polarity, the length of modifying time, and the total electrical charge that passed during electrochemical modification.

In this work, larger size (10 mm × 10 mm) $SrTiO_3$ substrates were used for electrochemical modification and the number of gold-STO contacts were varied to test for the ability to spatially pattern rutile TiO_2 particles on STO. Eighteen (10 mm × 10 mm) STO samples were subjected to electrochemical treatments similar to the ones applied to the smaller substrates. When the STO working electrode was clipped with a single alligator clip, anodic currents were measured, albeit at levels that were lower than ones found in our previous work. While darkening of the electrodes in the areas of contact was visually observable, no rutile TiO_2 crystals were found on the surface as verified by XRD. When anodically polarized, the STO working electrodes clipped with two alligator clips showed an unusual behavior, passing cathodic currents during the entire modification period. While such behavior is not fully understood, it has been found that the polarity of the current correlated with the level to which the electrodes were dipped in 1 M NaOH electrolyte such that the direction of the electrical current switched from cathodic at low levels of submersion to anodic when the STO electrodes were more deeply immersed into

the electrolyte. It should also be noted that the magnitude of the cathodic current was sometimes not very different from the one that corresponded to the instrument background (measured by short circuiting the cell by detaching the potentiostat lead from the working electrode).

Table of contents

Appendix: Tables and Figures of the Section Results and Discussion

Introduction

$SrTiO_3$ (strontium titanate, also called as STO) has attracted great interest of many researchers in recent decades due to its electrical properties and extensive applicability. It has been widely used as a substrate for thin-film photocatalysts,[1] high temperature superconductors[2,3] and oxygen sensors.[4] The fabrication procedures employed in many of these studies requires oxidation or reduction of the substrates and is often carried out at high temperature[5] in highly oxidizing or reducing environments.

Structure of $SrTiO_3$ and Rutile TiO_2

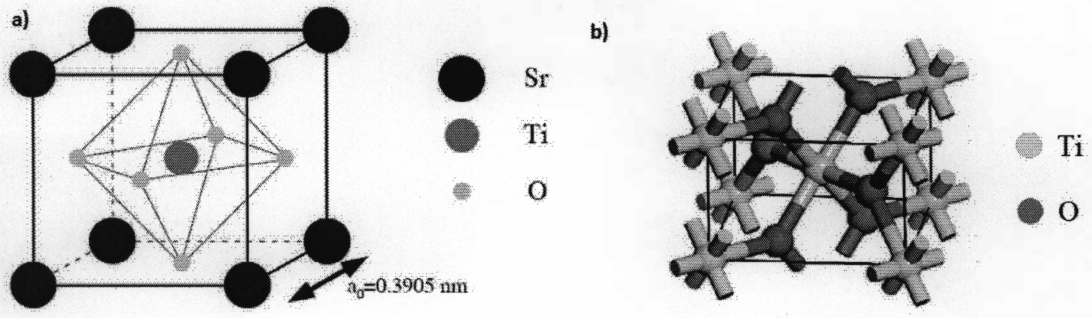

Figure 1. Atomic structure of $SrTiO_3$ (a) and rutile TiO_2 (b).

$SrTiO_3$ is a mixed metal oxide of perovskite-type structure typically labelled as ABO_3. The structure of the oxide is cubic and is shown in Figure 1a. The atom at the center of the cubic unit is a Ti^{4+} cation coordinated by six O^{2-} anions located at the center of each face forming a TiO_6 octahedral structure. The Sr^{2+} cations are located at the corners of the cube such that each is surrounded with four TiO_6 octahedra. The interaction between Ti^{4+} and O^{2-} exhibits covalent bonding character[6] giving $SrTiO_3$ features of both ionic and covalent compounds.

In the tetragonal unit cell of rutile TiO_2 shown in Figure 1b, each Ti^{4+} cation is surrounded by six oxygen anions and forms TiO_6 octahedral. Each oxygen anion is coordinated by three Ti^{4+} cations in a trigonal planar structure. The TiO_6 octahedra exist in the structures of both $SrTiO_3$ and TiO_2, indicating that the conversion between these two substances is feasible by applying appropriate experimental methods. Our goal of this project is to probe an electrochemical method for growth of rutile TiO_2 on $SrTiO_3$ substrates.

Oxygen Vacancies in $SrTiO_3$

At each temperature, there is an equilibrium of defects in the STO structure. These include oxygen vacancies, interstitial atoms and other cation vacancies. Most abundant are usually the oxygen vacancies which are, in most cases found to be the reactive sites on the surface of other mixed metal oxides and are responsible for their photoactive or conductive behavior. Oxygen vacancies in $SrTiO_3$ can be generated by heating in a reducing gas such as 20% H_2 at 1200 ℃.[7] Such treatment may result in a change of the structure by removing oxygen from the substrate surface causing the TiO_6 octahedra to twist to a square pyramid or tetrahedron. Doping the STO with small amounts of other transition metals is another common method to generate oxygen deficient perovskite materials. For instance, $Sr_nTi_mFe_{n-m}O_{3n-1}$ can form by partially replacing Ti^{4+} with Fe^{3+}. This introduces a charge imbalance which can partially be compensated by forming oxygen vacancies, by iron attaining a higher oxidation state or both.[8] This, in turn, increases the overall conductivity of the STO.

Incorporation of Oxygen in $SrTiO_3$

The thermodynamic and kinetic studies of the reactions between gas phase O_2 and $SrTiO_3$ material revealed that there are three steps of oxygen incorporation into $SrTiO_3$. These include surface reaction, chemical diffusion into the bulk and moving inside the bulk along grain boundaries.[9,10]

The surface reaction in the gas phase includes adsorption of molecular oxygen, electron transfer to or from the oxygen molecule, dissociation of the O-O bond, and incorporation of oxygen ions into the oxygen vacancies.[10] After oxygen gas is adsorbed on the surface of $SrTiO_3$, the molecule of oxygen is converted to O_2^- by gaining an electron from the conduction band of $SrTiO_3$ material. A second electron transfer occurs in the same way, where O_2^- becomes O_2^{2-}, which rapidly splits into two O^- anions that is considered as the only oxygen species that can fill into the oxygen vacancies of the STO.[10]

After the oxygen species have been incorporated into the first surface and sub-surface layers of the STO, they move further into the bulk driven by chemical diffusion. For polycrystalline STO substrates, it is at the grain boundaries that their concentration was found to rise abruptly as their motion was suppressed by higher energy barriers in these regions. Further diffusion of oxygen species takes place along the path of least resistance – along the grain boundaries rather than by diffusing between different grains.[11]

Wet electrochemical treatment in alkaline solutions has also been found to produce similar incorporation effects.[8] These treatments have usually been performed at room temperature, at potentials immediately prior to oxygen evolution. For sufficiently long

modification times, the electrochemical treatment has been found to result in entirely new phases which have been detected by x-ray diffractometer.[12]

Motivation

Our previous work[12] revealed that anodic polarization of STO (100) substrates in 1 M NaOH lead to the formation of rutile TiO_2 crystals in the area of contact between the STO working electrode and the Au-coated alligator clip. The amount and density of the crystals was found to depend on the potential, time of polarization and the overall electrical charge that passed during the experiment. This work is motivated by our wish to investigate whether it is possible to guide the crystal growth by appropriate positioning of two contacts on a single STO substrate thereby spatially patterning TiO_2 crystals on STO. In order to enable positioning of two contacts on a single STO working electrode, we used (10 mm × 10 mm) $SrTiO_3$ substrates instead of the smaller (5 mm × 5mm) electrodes used in our previous work.[12]

Literature review

The combination of TiO_2 and $SrTiO_3$ called a $SrTiO_3/TiO_2$ heterojunction was extensively applied into the design for new photoelectrochemcial materials. Compared with bare TiO_2 electrodes, these materials exhibit higher charge transfer speed, better surface-dominant photoelectrochemical response and higher photon-to-current conversion efficiency.[13] It was reported that the dye-sensitized solar cell design with $SrTiO_3/TiO_2$ heterojunction anode exhibits an increased photovoltage due to the fact that charge recombination at the TiO_2/dye/electrolyte interface was suppressed by the matched band potential of STO.[14] $SrTiO_3/TiO_2$ heterojunction nanotubes were also found to be good photocatalysts in the H_2 evolution reaction in the overall splitting of water.[15] In another application, this composite material also showed higher photocatalytic activity in the destruction of organic dyes, which makes it a promising candidate for photochemical pollutant decomposition.[16]

To employ this design into an operating device, various fabrication technologies have been used. The most common one is hydrothermal synthesis which partially converts $SrTiO_3$ to TiO_2 on the surface of $SrTiO_3$ substrate.[17] This technology requires conditions where the STO is exposed to a high temperature placed at high-temperature and vapor pressure. Atomic layer deposition (ALD) also is a widely-used method to grow epitaxial layers of TiO_2 and $SrTiO_3$ upon various substrates.[18] In addition, electrospinning[19] and high temperature annealing[20] were used to develop nanodevices of $SrTiO_3/TiO_2$ heterojunctions for various purposes and worked successfully. These technologies require harsh working conditions such as high temperature[21] (up to 3000 °C), high pressure or special instrumentation.

Our previous work has shown that 5 mm × 5 mm $SrTiO_3$ substrates in 1 M NaOH solution show similar oxidation plateaus at potentials preceding the oxygen evolution (0.5 - 0.6 V vs. Hg/HgO).[12] Oxygen evolution currents were observed at potentials higher than 1.2 V, while applying a constant positive potential (in the range of 0.6 - 1.2 V) for several hours resulted in the formation of new phases in the interfacial areas of contact between gold and STO. These experiments were performed potentiostatically and the resulting current decay curves resembled the ones that are often seen with electrochemical reactions accompanied by diffusion.[22]

The surface change of the modified substrates was confirmed by both naked-eye observation and the surface topographies obtained by using atomic force microscopy (AFM).[12] It has been found that the surface of the substrate was darkened and the darkening was only presented in the area where a gold coated clamp used for connection clipped. The surface topological examination by atomic force microscopy (AFM) revealed the presence of triangular crystals while these crystals were identified as rutile TiO_2 by XRD.

Experimental

Materials

$SrTiO_3$ (100) (5 mm × 5 mm and 10 mm × 10 mm) one-side-polished substrates were purchased from MIT Corporation (Richmond, California, USA) and used as working electrodes. Sodium hydroxide pellets (semiconductor grade, 99.99% trace metal basis) were provided by Sigma-Aldrich Corporation (St. Louis, Missouri, USA). Acetone (HPLC grade, $\geqslant$ 99.9%) and 2-propanol (LC-MS chromasolv) were purchased from Sigma-Aldrich Corporation (St. Louis, Missouri, USA). Nochromix crystals were purchased from Godax Laboratories, Inc. (Cabin John, MD, USA). Sulfuric acid (98%) was purchased from Fisher Scientific (Pittsburg, PA, USA).

Hg/HgO (20% KOH) was used as a reference electrode (RE) (CHI Instruments, Inc., Austin, Texas, USA). Ag/AgCl (3 M NaCl) reference electrode was only used for the experiments to check working conditions or troubleshooting. Unless otherwise stated, all potentials in this thesis are referred to Hg/HgO RE.

Solutions of 1 M NaOH were prepared by dissolving the NaOH pellets in 10 MOhm Millipore water. Nochromix solution was prepared by dissolving the Nochromic crystals into concentrated sulfuric acid. Prior to use, all glassware as well as the Pt-wire counter electrode (CE) were cleaned by soaking in Nochromix solution for at least 12 hours.

Instrumentation

Two potentiostats were used for electrochemical measurements: CHI-660C and CHI-731E, both from CH Instruments (Austin, Texas, USA).

Methods

Before electrochemical modification the substrates were sonicated for about 5 minutes in each of three solvents in the following order: acetone, 2-propanol and Millipore water. The substrates were dried by natural convection in air after which they were clipped using gold-coated alligator clips (Pomona Electronics, Everett, WA), making a single- (Figure 2b) or a double-contact (Figure 2c) working electrode (WE). The electrochemical cell was a single-compartment glass cell. The relative position of the WE, RE and CE electrodes in the cell during electrochemical measurements is shown in Figure 2a.

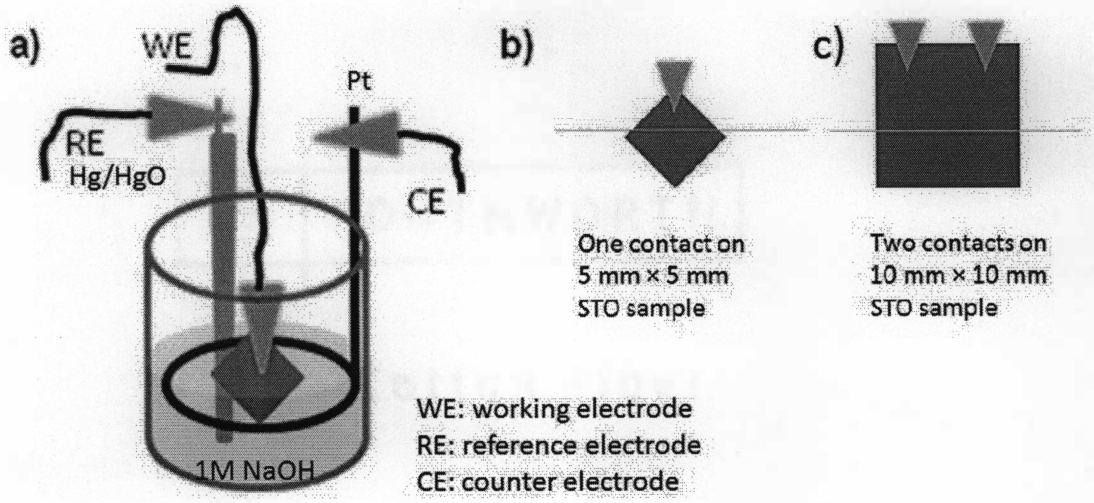

Figure 2. Illustration of the setup of the electrodes a) and the manner in which the STO substrates were clipped with one b) and two c) alligator clips.

After the WE, CE and RE were immersed in the electrolyte, the WEs were polarized anodically by applying a chosen potential in the region between 0.8 V and 1.7 V for different amounts of time during which the current was continuously monitored. Depending on the duration of the experiment, data points were taken every 1 or 30 seconds.

After the experiment, the WE was taken out of solution, rinsed with Millipore water and visually inspected for the presence of darkened areas around the gold-STO contact.

The electrochemical setup shown in Figure 2 was also used for measuring the background signal except that, in this case, the WE was removed from the electrolyte and the WE potentiostat lead disconnected from the Au-coated alligator clip. The potential was then cyclically scanned from 0 V to 1.2 V at a scan rate of 0.1 V/s. These background current measurements were performed by cyclic voltammograms at various current sensitivity levels.

Several cyclic voltammograms were recorded using Pt-wire as a working electrode. These experiments were performed either in 1 M NaOH or 0.5 M H_2SO_4 solutions.

The data were collected as .txt files by the CHI software, after which they were imported into and plotted by Sigmaplot 12.0 software.

Results and Discussion

Summary of Results for the Electrochemically Treated Substrates

Tables 1, 2 and 3 summarize the experimental conditions and the polarity of the currents measured during the experiments with (5 mm × 5 mm) (Table 1) and (10 mm × 10 mm) STO substrates (Table 2 and Table 3). The approximate levels to which the electrodes were immersed as well as the presence or absence of darker areas in the region of Au-STO contacts were also recorded. Nine out of ten (5 mm × 5 mm) substrates exhibited anodic currents and 8 out of 10 resulted in having darker areas. Both observations are consistent with the results we have obtained in our previous studies.[12] A switch from cathodic to anodic currents was observed with one of the substrates after the first 649 seconds of anodic polarization at 1.2 V vs Hg/HgO. While the reproducibility of the (5 mm × 5 mm) substrate measurements was not equal to 100%, taken together, the data in Table 1 do show that anodic polarizations result in anodic currents and that, the darkening due to the presence of new phases near the contact area usually appears when anodic current are observed.

In an attempt to spatially pattern the darker areas on larger (10 mm × 10 mm) STO substrates, a number of (10 mm × 10 mm) substrates were polarized anodically at several potentials in the range between 1.0 V and 1.7 V. Experiments were performed with setups that used either single or double Au-STO contacts. The position of the Au-STO contacts is schematically depicted in Figure 2b for a single and Figure 2c for a double contact.

A summary of the results of these studies is shown in Table 2 and 3. The data in Table 2 show that the 10 mm × 10 mm STO substrates, when anodically polarized at

constant potential exhibit anodic currents only when a single Au-STO contact is used. Having two Au-STO contacts almost always resulted in negative (i.e. cathodic) currents (Table 3). We didn't observe darkened areas on any of these samples.

In Table 4, cyclic voltammetry experiments of these substrates always resulted in negative currents. The orders of magnitude of current strength are lesser than the ones of the corresponding sensitivities by 3 in most cases, only different one was the result ran on another potentiostat CHI-731E. This discovery also can be found in previous tables when the negative current showed up.

The amperometric i-t curves obtained in these experiments were quite irreproducible and varied between different substrates or the different experiments on a single substrate. Figure 3 - 13 show i-t curves obtained with 5 mm × 5 mm substrates clipped with one alligator clip. It can be seen that upon anodic polarization the currents varied in polarity as well as in whether they were rising or decaying over time. Negative current values were observed after long time experiments (Figure 9 and 12) due to the evaporation of the supporting electrolyte solution, and it turned back to positive after the compensation of the supporting electrolyte was made (Figure 9).

Figure 14 - 26 show i-t curves of 10 mm × 10 mm substrates with both one- and two-contact. As we can see, negative current was more often observed in two-contact setting. The trends of the currents were increasing while negative values showed up.

The cyclic voltammogram shown as Figure 27 - 33 all locate in negative region. However, the pattern of them are quite different, some are noise-like, a bunch of random dots in a range of negative values (Figure 29, 31, 32), and others (Figure 27, 28, 30) did

show some features of the cyclic voltammogram of previous work[8,12], like an oxidation plateau at 0.6 V in Figure 27.

"Negative" Values of Currents

When 10 mm × 10 mm $SrTiO_3$ substrates were clipped with two gold coated clamps and set as the working electrode for electrochemical modification by exposure to positive potential, we observed negative current during the treatment in most cases. In addition, no darkening was found on these substrates surface, no crystals were formed in clipped area. While the reasons for such behavior are not fully understood, we note that abrupt changes in current levels have previously been observed during electrochemical modification of a number of non-stoichiometric oxides[23] and are usually explained by abrupt changes in conductivity due to changes in the degrees of non-stoichiometry (i.e. concentration of oxygen vacancies, changes in oxidation states of the transition metals as well as the segregation and formation of new crystalline phases).[24]

Based on the results all above, we can address the observation in summary as following: The negative current was observed in most cases when 10 mm × 10 mm $SrTiO_3$ substrates were introduced with one- or two-contact setup, and the orders of magnitude of these current values are various from 10^{-4} to 10^{-7}. All these results were represented as noise-like curves indicating the data was severely affected by noises or errors. Some results were just numerous dots were densely compacted in a negative value band, and the others have some kinds of familiar behavior as the results of 5 mm × 5 mm substrates we used before, like the cyclic voltammogram with an oxidation plateau (Figure 27), or an amperometric i-t curves show the trends of the currents strength continuously increasing (Figure 23 - 26) or decreasing (Figure 18, 19, 21) and then turn to a relatively steady level.

The observation of these results brought out more challenging questions: since there is no spontaneous reaction between the working electrode ($SrTiO_3$) and the electrolyte (1 M NaOH), the negative current values does not mean actual reverse current in such experiments. Would this negative current indicate no current was detected and only the background signal was recorded and displayed in the results? And why did some curves have some features of previous works, if there is no current passed though the circuit and the background signal is very unlikely able to show it. However, the most important question is why do larger substrates pattern so different from our previous work with smaller substrates. Therefore, further experiments will be designed to clarify the findings.

Troubleshooting

The presence of cathodic currents upon anodic polarization in electrochemical experiments usually indicates that one or more of electrical contacts within or outside of the electrochemical cell are malfunctioning. Much time was devoted to troubleshooting these observations. First, the working electrode was changed from STO to Pt wire and CVs of Pt wire were recorded in both 0.5 M H_2SO_4 and 1 M NaOH electrolytes (Figure 34, 35). Next, an experiment with a different reference electrode (Ag/AgCl instead of Hg/HgO) was performed (Figure 36), the potential scanning technique was changed from that of "cyclic voltammetry" to the "sweep-step technique" (Figure 37), the WE was detached from the electrical circuit and potential applied (Figure 38 and 39). These troubleshooting experiments showed that the negative current occurred in all cases except when the STO WE was replaced with a Pt wire. It indicated that the negative current originated from the STO-WE and/or the Au-STO contact.

Because, it was observed that the direction of current would vary between positive and negative values the depth to which the WE was immersed varied from experiment to experiment, a series of amperometric experiments with varying levels of immersion of STO into the electrolyte were performed and these data are shown in Figure 40 - 42. Furthermore, same experiments performed with different concentration of the supporting electrolyte (Figure 43 - 48).

Another potentiostat CHI-731E was used to verify the results of some experiments performed before (Figure 49 - 51).

Cyclic Voltammograms of Platinum in Acidic and Alkaline Solutions

Cyclic voltammetry is considered as a powerful and sensitive method to investigate electrochemical properties of the electroactive materials.[24] The characteristic cyclic voltammogram of platinum is most likely the best known of all materials and can be used as a standard curve for checking electrochemical experiment conditions. Figure 34 is the cyclic voltammogram of a platinum electrode in 0.5 M H_2SO_4 solution. As we can see, there are two distinct peaks referring to the hydrogen deposition located in the range of -0.1 ~ -0.2V, and a plateau at 1.2 V indicates the platinum oxidation, and an inverse peak regarding to platinum reduction is at 0.5 V. This result matches the cyclic voltammogram obtained by previous researchers[25] (Figure 56), and is strong evidence for the good status of our working conditions.

The cyclic voltammogram of a platinum electrode in 1 M NaOH (shown as Figure 35) is a little different from the previous acidic one. First, the potentials of the peaks were shifted slightly due to the pH change. The three distinct peaks of hydrogen deposition were

move to in the range of -0.5 ~ -0.8 V, and the inverse peak of platinum reduction was found at -0.3 V. However, there is no obvious peak or plateau indicating the oxidation of platinum for unknown reason.

Replacement of Reference Electrode from Hg/HgO to Ag/AgCl

This attempt was trying to investigate the effect of reference electrode in electrochemical modification. Therefore, Ag/AgCl reference electrode was used instead of Hg/HgO RE only for a short time (5 mins) experiment because Ag/AgCl RE is unstable and can be ruined in alkaline electrolyte. The result shown in Figure 36 is a noise-like dots in negative region, which referring that the reference electrode was not responsible for negative current.

Sweep-step Technique

Sweep-step experiment is basically a way to cycle the potential with successively increasing the anodic limit by 0.2 V. Basically, that experiment should show what happens to the surface as it is progressively polarized by more positive potentials.

The result shown in Figure 37 is a curve locates in negative region, and the values of current was increasing with running time instead of the applied potential.

Background Signal Tests

$SrTiO_3$ is stable in common alkaline solution like 1 M NaOH, which means that there will be no spontaneous reaction between them. Thus, the background signal is the one mostly likely be responsible for the occurrence of negative current. To verify this theory, detached the working electrode from the setup, to make the whole setup as an open

circuit, then run cyclic voltammetric scanning. It is assumed that no current will pass through the circuit for the reason discussed before, thus the results would only represent the background signal. We tested the background signal levels on both potentiostats for each sensitivity level from 1×10^{-1} to 1×10^{-9} A/V, and two of them are presented in Figure 38 and 39.

As we can see, the background signal is presented as the indented, rough curves with negative current values, and they are about three orders of magnitude lesser than the corresponding sensitivity levels which also can be observed from previous results in which negative current were found.

It is clear now that the source of the so called negative current was the background signal of the potentiostat. We can then speculate that the reason for background-signal-like results is because there was no actual current or very weak current passed through the circuit. Furthermore, if the strength of current and background signal are at the similar level, the current would shift into the negative region, but it could show some similar pattern as our previous works.

Effect of Immersion Depth on the Cyclic Voltammetry of $SrTiO_3$ Substrates

As we discussed before, the 10 mm × 10 mm $SrTiO_3$ substrates show very different conductivity from the 5 mm × 5 mm substrates in similar conditions and operations. However, difference in the submergence level of substrates had not been studied. The submergence levels of the10 mm × 10 mm substrates were varied compared to the 5 mm × 5 mm substrates since they have larger size. Therefore, the experiments designed to probe

the relationship between conductivity and submerging levels was carried out, and the results were shown in Figure 40, 41 and 42.

All these experiments were performed running cyclic voltammogram with one contact on 10 mm × 10 mm substrates submerging in electrolyte at three levels illustrated on the right side of each figure: least, near half, and over half. It was clear that the substrates submerged at first two levels were found insulate since 40 and 41 are just background-signal-like curves and no positive current was detected. However, the result in Figure 42 corresponding to the substrate being submerged into the electrolyte more than half of its area was that the positive current occurred shortly after the experiment started. It is mentioning that the strength of the current is not proportional to the submerged area size of the substrates, and that the anodic current only abruptly show up after more than half of substrates were immersed. This result is surprising because in most electrode material the conductivity of the working electrode is proportional to the contact (submerged) area in most cases.

Effect of Concentrations of Electrolyte.

To investigate if the concentration of the electrolyte could affect the conductivity of the substrates, similar conductivity tests were performed in different concentration of NaOH solutions. Figure 43, 44, 45 represent the results of conductivity tests ran in 0.5 M NaOH solution, and Figure 46, 47, 48 are the results of same experiments ran in 2 M NaOH solution, and each submerged level is illustrated on the right side of each diagram.

Based on these results shown in Figure 43 - 48, we conclude that different concentrations of electrolyte have no effect on the conductivity of the substrates. All the

results with substrate submerging levels of least or near half are background-signal-like curves with negative values and positive currents are only obtained while the substrate was dipped more than half of size.

Verification of the CHI-660C by Comparing with CHI-731E Potentiostat

To make sure that there is same instrumental error in experiments, we ran background signal tests on another potentiostat CHI-731E at sensitivity level from 10^{-1} to 10^{-7} A/V, and two of the results were shown as Figure 49 and 50. The behavior of CHI-731 in such experiments are similar to the ones of CHI-660C we used before, the background signal is noise like dots in negative region, and it is more close to zero at high sensitivity level like 10^{-7} A/V.

Another cyclic voltammogram on a 10 mm × 10 mm $SrTiO_3$ substrate with two contacts and least submerged level also ran on the potentiostat, CHI-731E, and the result is presented in Figure 51. This result shows us that there is no current and only background signal was detected by the new potentiostat during the experiment, and that it is well-matched to the results obtained from the potentiostat CHI-660C. Thus, the potentiostat was not responsible for the negative current.

Cyclic Voltammetry of $SrTiO_3$ Substrates

The discovery about background signal brought us a new question: what caused such a big difference in conductivity between the 5 mm × 5 mm $SrTiO_3$ substrates used in previous work and the 10 mm × 10 mm substrates introduced recently. Therefore, a series of experiments for conductivity tests were performed.

The cyclic voltammetry on both of two types of substrate was conducted for conductivity tests by clipping two ends of the substrates with working electrode and counter electrode leads. In the results shown in Figure 52 and 53, we found that both are insulators since only background signal was recorded in the diagrams. This observation was supported by some statements in the lieratures[26,27] that $SrTiO_3$ has a wide band gap and is an insulator at room temperature. Therefore, submerging the substrates into 1 M NaOH solution is essential for making the substrate conductive and electrochemically modified.

Effect of Excessive Immersion of STO Substrate

We clipped a 5 mm × 5 mm $SrTiO_3$ substrate with one clamp and dipped it into 1 M NaOH as much as possible, and the current was positive during whole process when a positive potential was applied. However, no darkened spots were found in clipped area, indicating that no TiO_2 crystals were produced compare to results in Table 1. The reason is not clear yet, but it is very possible that because the substrate was submerged too much, and the clamp is too close to the electrolyte, even though they were not touched each other from naked eye observation, and the crystals could not form because the reaction might not actually happen under such conditions. This theory is supported by comparing the cyclic voltammogram of this STO substrate (shown as figure 54) with the cyclic voltammogram of a gold-coated clamp (shown as Figure 55).

Figure 55 was obtained while the gold coated clamp was dipped into the electrolyte without any other material clipped. As we can see, the shapes of two curves between 0 ~ 0.6 V are similar, and the location of the characteristic inverse peaks are same. We conclude that the gold coated clamp reached the electrolyte during the experiment eventhough we

could not observe by using naked eyes. Therefore, the current most likely directly passes through from the clamp to the electrolyte without the participation of the $SrTiO_3$ substrate. No crystals were formed since no current passed though the substrate and no reaction happened.

Conclusion

Regarding that negative current was observed during the electrochemical experiments carried out on new larger size $SrTiO_3$ substrates, a comprehensive investigation was conducted to find out the reason for this unexpected behavior of the new substrates. First, the background signal tests were carried out for each sensitivity by running cyclic voltammetric scanning after disconnecting the working electrode lead from the circuit. Thus, it was clear that the negative current values actually were caused by the background signal of the potentiostat if there was no current or very weak current passed through the circuit. Then the conductivity tests on dry $SrTiO_3$ substrates confirmed that dry $SrTiO_3$ is an insulator and it needs to be dipped into 1 M NaOH solution to participate in the reaction.

Further explorations were focused on the relationship between the submerging levels and the conductivity of the substrates. The results showed us that the positive current only occurred when the substrate was submerging into the electrolyte at appropriate level, otherwise there was no real current but background signal observed. And similar experiments ran with various concentration of electrolyte proved that the concentration of electrolyte has no apparent effect on the conductivity of the substrates. However, the probe into an electrochemical modification on a substrate was most submerging level into the electrolyte exhibits that the TiO_2 crystals could not formed with an excessively submerging level of substrate because the gold coated clamp and the surface of electrolyte solution were found to have touched each other.

The most important conclusion we must point out is that the strength of the current has no proportional relationship to the size of submerged area of the substrate, which is unusual for the materials used as working electrode in electrochemical research. And there was an interaction between the $SrTiO_3$ working electrode and electrolyte to trigger $SrTiO_3$ substrate conductivity then participate the reaction to form TiO_2 crystals upon the surface of the substrate, but the mechanism of this interaction is not revealed yet and it could be a goal of our future work.

Suggestion for Future Work

Our future research could focus on the interaction between the $SrTiO_3$ substrates and the electrolyte solution which changed the conductivity of the substrates. Its mechanism still is unclear, but there is a hypothesis can explain the most of observations and the results, and of course it needs to be test by further experiments. Wetting is a very common phenomenon occurred on solid surface while solid is immersed into liquid, and it most likely will happen on the STO substrate surface in our experiments, and it might be the prerequisite of the interaction which changed the conductivity of the $SrTiO_3$ substrates at the appropriate submerging level. It can explain why the cyclic voltammogram of the substrate excessively submerged is very like the cyclic voltammogram of the gold coated clamp, and supported by our previous observation that the most significant changes of the percentages of the elements were occurred at the edge instead of the center of the clipped area, and the formed TiO_2 crystals were just loosely adhered on the surface of the substrate and can be easily removed by sonication. However, it requires a delicate design of experiment to verify this hypothesis.

Another improvement for this project can be made by replacing the substrate from STO to transition-metal-doped STO, like Fe- or Nb-doped STO. This kind substrates provide better conductivity for the electrochemical modification, and thus no need to consider the depth of immersion of the substrates in electrolyte, while the depth of immersion was not reproducible in experiments.

References

1. Hara, S.; Yoshimizu, M.; Tanigawa, S.; Ni, L.; Ohtani, B.; Irei, H. *J. Phys. Chem. C* **2012**, *116*, 17458-17463.
2. Stornaiuolo, D.; Gariglio, S.; Couto, N. J. G.; Fete, A.; Caviglia, A. D.; Seyfarth, G.; Jaccard, D.; Morpurgo, A. F.; Triscone, J.-M. *Applied Physics Letters* **2012**, *101*, 222601/1-222601/4.
3. Takahashi, K. S.; Matthey, D.; Jaccard, D.; Triscone, J.-M.; Shibuya, K.; Ohnishi, T.; Lippmaa, M. *Applied Physics Letters* **2004**, *84*, 1722-1724.
4. Neri, G.; Micali, G.; Bonavita, A.; Licheri, R.; Orru, R.; Cao, G.; Marzorati, D.; Merlone Borla, E.; Roncari, E.; Sanson, A. *Sensors and Actuators, B: Chemical* **2008**, *134*, 647-653.
5. Hu, Y.; Tan, O. K.; Cao, W.; Zhu, W. *Proceedings of IEEE Sensors 2003. IEEE International Conference on Sensors, 2nd, Toronto, ON, Canada, Oct. 22-24, 2003* **2003**, *2*, 1305-1309.
6. Leapman, R. D.; Grunes, L. A.; Fejes, P. L. *Phys. Rev. B* **1982**, *26*, 614-635.
7. Moos, R.; Menesklou, W.; Hardtl, K. H. *Appl. Phys. A* **1995**, *61*, 389-395.
8. Grenier, J. C.; Wattiaux, A.; Fournes, L.; Pouchard, M.; Etourneau, J. *J. Phys. IV France* **1997**, *7*, 49-52.
9. Merkle, R.; Maier, J. *Angew. Chem. Int. Ed.* **2008**, *47*, 3874-3894.
10. Merkle, R.; Maier, J. *Phys. Chem. Chem. Phys.* **2002**, *4*, 4140 –4148.
11. Maire, J.; Jamnik, J.; Leonhardt, *Solid State Ionics* **2000**, *129*, 25-32.
12. Harmon, K. J. M. S. Thesis, Eastern Illinois University, Charleston, IL, 2013.
13. Yukawa, R.; Yamamoto, S.; Ozawa, K.; D'Angelo, M.; Ogawa, M.; Silly, M. G.;

Sirotti, F.; Matsuda, I. *Physical Review B: Condensed Matter and Materials Physics* **2013**, 87, 115314/1-115314/6.

14. Chao, Z.; Wang, C.; Li, J.; Kun, Y. *Chinese Physics* **2007**, *16*, 1422-1428.
15. Guo, L.; Wang, X.; Zhang, H.; Li, L. *Ceramics International* **2013**, *39*, 633-636.
16. Wang, Y.; Chen, T.; Huang, Y.; Huang, T.; Lee, Y.; Chiu, H.; Lee, C. *Journal of the Chinese Chemical Society (Weinheim, Germany)* **2013**, *60*, 1437-1441.
17. Su, E.; Huang, B.; Wey, M. *Solar Energy* **2016**, *134*, 52-63.
18. Khalyavka, T. A.; Kamyshan, S. V.; Tsyba, N. N. *Ukrainskii Khimicheskii Zhurnal*, **2016**, *82*, 27-30.
19. Zhou, J.; Yin, L.; Li, H.; Liu, Z.; Wang, J.; Duan, K.; Qu Shuxin; Weng J.; Feng, B. *Materials Science in Semiconductor Processing* **2015**, *40*, 107-106.
20. Kraus, T. J.; Nepomnyashchii, A. B.; Parkingson, B. A. *Journal of Vacuum Science and Technology, A: Vacuum Surfaces, and Films* **2015**, *33*, 01A135/1-01A135/6.
21. Bai, H.; Liu, Z.; Sun, D. D.; *Journal of American Ceramic Society* **2013**, *96*, 942-949.
22. Oropeza, F. E.; Zhang, K. H. L.; Regoutz, A.; Lazarove, V. K.; Wermeille, D.; Poll, C. G.; Egdell, R. G. *Crystal Growth and Design* **2013**, *13*, 1438-1444.
23. Deak, D. S.; Silly, F.; Newell, D. T.; Castell, M. R. *Journal of Physical Chemistry B* **2006**, *110*, 9246-9251.
24. Kissinger, P. T; Heineman, W. R. *Journal of Chemical Education* **1983**, *60*, 702-706.
25. Daubinger, P.; Keininger, J.; Unmussig, T.; Urban, G. A. *Phys. Chem. Chem. Phys.* **2014**, *16*, 8392-8399.

26. Kumar, S. R. S.; Barasheed, A. Z.; Alshareef, H. N. *ACS Appl. Mater. Interfaces* **2013**, *5*, 7268-7273.

27. Noland, J. A. *Physical Review*, **1954**, *94*, 724–724.

Appendix: Tables and Figures of the Section Results and Discussions

(Most experiments were carried out in 1 M NaOH solution as supporting electrolyte unless specified other electrolytes were using in the captions)

Table 1: Results of electrochemical modified 5 mm × 5 mm substrates

Sample #	Potential (V)	Time (hours)	Depth of immersion	Sensitivty (A/V)	Current level (A)	Darkening
09/06/13 01	1.2	1	N/A	10^{-3}	6.5×10^{-3}	Yes
09/19/13 01*	1.2	2	N/A	10^{-3}	-2×10^{-6}, 8×10^{-3}	Yes
140709-01	1.2	1	N/A	10^{-1}	6×10^{-3}	Yes
140709-02	1.2	1.5	N/A	10^{-1}	1.4×10^{-3}	Yes
140710	1.2	2	N/A	10^{-1}	8×10^{-4}	Yes
150807-01	0.8	2	N/A	10^{-3}	2×10^{-5}	No
20160126	1.0	20	Over half	10^{-3}	3×10^{-4}	No
20160128	1.0	18	Half	10^{-3}	1×10^{-5}	Yes
20160201	1.0	12	Half	10^{-5}	5×10^{-6}	Yes
20160204	1.0	8+10	Half	10^{-3}, 10^{-5}	5×10^{-4}, 5×10^{-6}	Yes

All 5 mm × 5 mm substrates were clipped as one contact. Starred sample (09/19/13 01) was observed negative current values (the first one in the cell) in first 649 seconds of electrochemical modification.

Table 2: Result of one-contact electrochemical modified 10 mm × 10 mm substrates

Sample #	Potential (V)	Time (hours)	Depth of immersion	Sensitivity (A/V)	Current level (A)	Darkening
140918	1.7	18	N/A	10^{-1}	-6×10^{-5}	No
140924	1.7	2	N/A	10^{-4}	5×10^{-6}	Yes
141001-01	1.7	2	N/A	10^{-4}	1×10^{-6}	Yes
141010-1	1.7	2	N/A	10^{-2}	1.6×10^{-4}	Yes
141103-1	1	2	N/A	10^{-4}	7×10^{-6}	Yes
141212	1.0	2	N/A	10^{-4}	2×10^{-6}	No

Table 3: Results of two-contact electrochemical modified 10 mm × 10 mm substrates

Sample #	Potential (V)	Time (hours)	Depth of immersion	Sensitivity (A/V)	Current level (A)	Darkening
140703	1.2	24+24	N/A	10^{-1},10^{-4}	-6×10^{-5}, -2×10^{-7}	No
140829-01	1.7	18	N/A	10^{-4}	5×10^{-6}	No
20140903-01	1.7	18	N/A	10^{-1}	-1.6×10^{-4}	No
20140908-01	1.7	18	N/A	10^{-1}	-1×10^{-4}	No
20140909-01	1.7	18	N/A	10^{-1}	-1.4×10^{-4}	No
20140916-01	1.7	18	N/A	10^{-1}	-2.5×10^{-4}	No

Table 4: Results of cyclic voltammograms of 10 mm × 10 mm substrates

Sample #	Contacts #	Potential (V)	Depth of immersion	Sensitivity (A/V)	Current polarity and level (A)
141202-01	1	CV	N/A	10^{-3}	(-) 10^{-6}
141203-01	1	CV	N/A	10^{-3}	(-) 10^{-6}
141216-01	1	CV	N/A	10^{-4}	(-) 10^{-7}
150808-01	1	CV	N/A	10^{-4}	(-) 10^{-7}
150816	1	CV	N/A	10^{-3}	(-) 10^{-6}
20160419	2	CV	Least	10^{-2}	(-) 10^{-7}

These substrates only ran cyclic voltammetric scanning for several minutes, and it is not long enough for darkening in contact area and forming crystals,

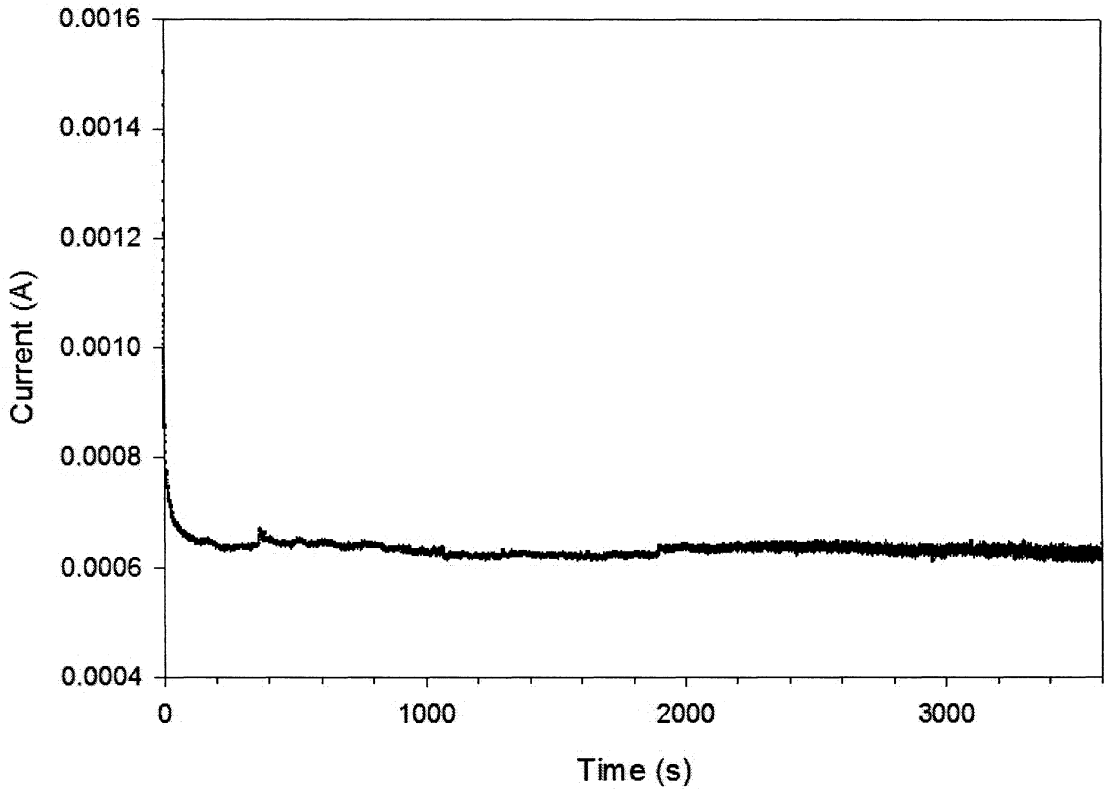

Figure 3. Amperommetric i-t curve of a 5 mm × 5 mm STO substrate (sample # 09/06/13 01) with one contact at 1.2 V vs. Hg/HgO for 1 hour. The sensitivity was 10^{-3} A/V.

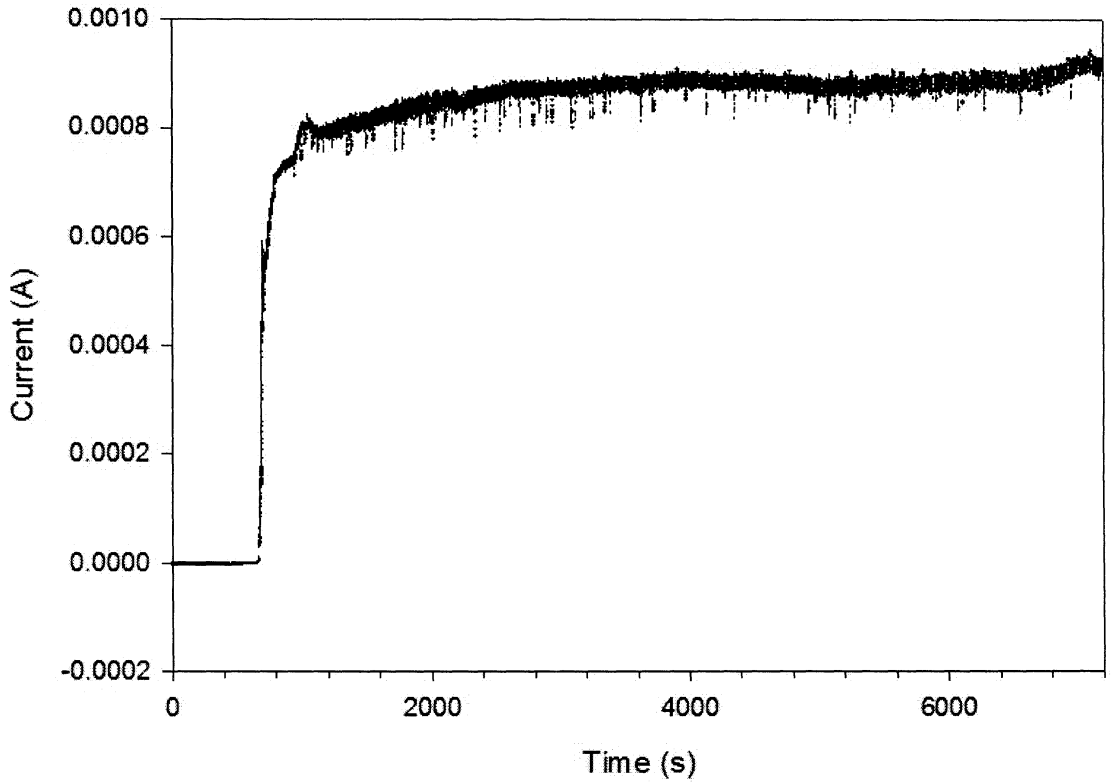

Figure 4. Amperommetric i-t curve of a 5 mm × 5 mm STO substrate (sample # 09/19/13 01) with one contact at 1.2 V vs. Hg/HgO for 2 hours. The sensitivity level was 10^{-3} A/V and negative current values (about -2×10^{-6} A) were found in first 649 seconds.

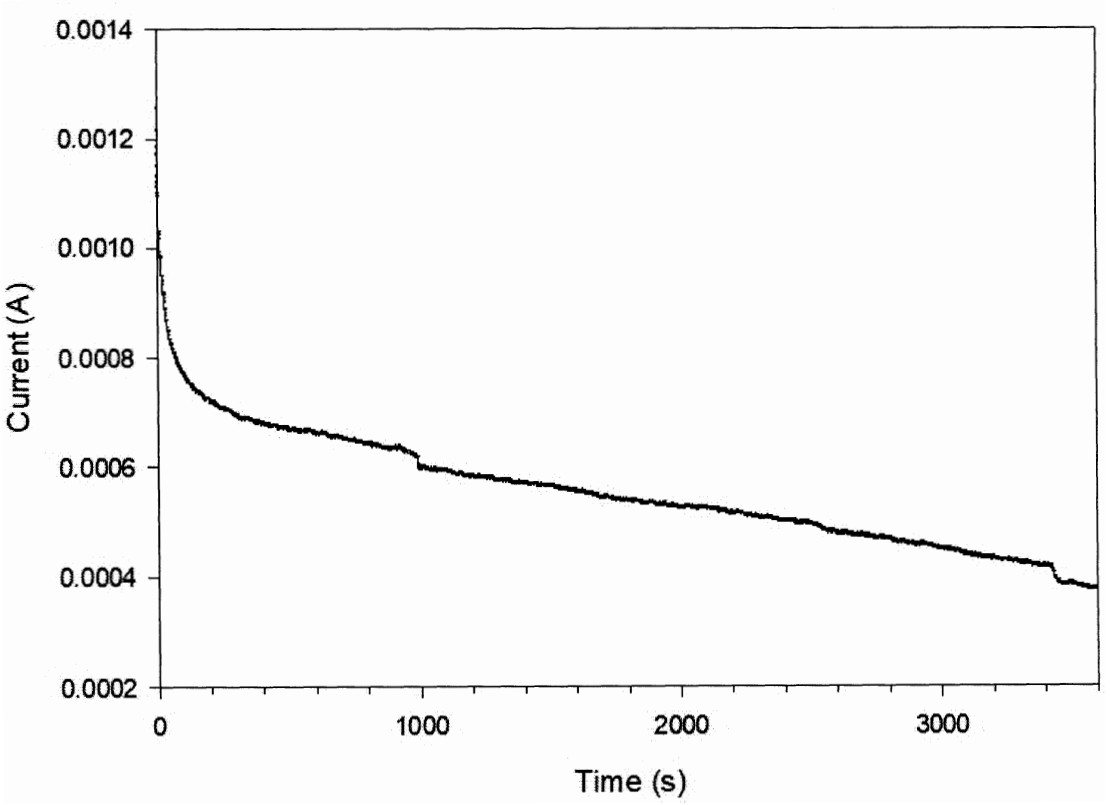

Figure 5. Amperommetric i-t curve of a 5 mm × 5 mm STO substrate (sample # 140709-01) with one contact at 1.2 V vs. Hg/HgO for 1 hours. The sensitivity level was 10^{-1} A/V.

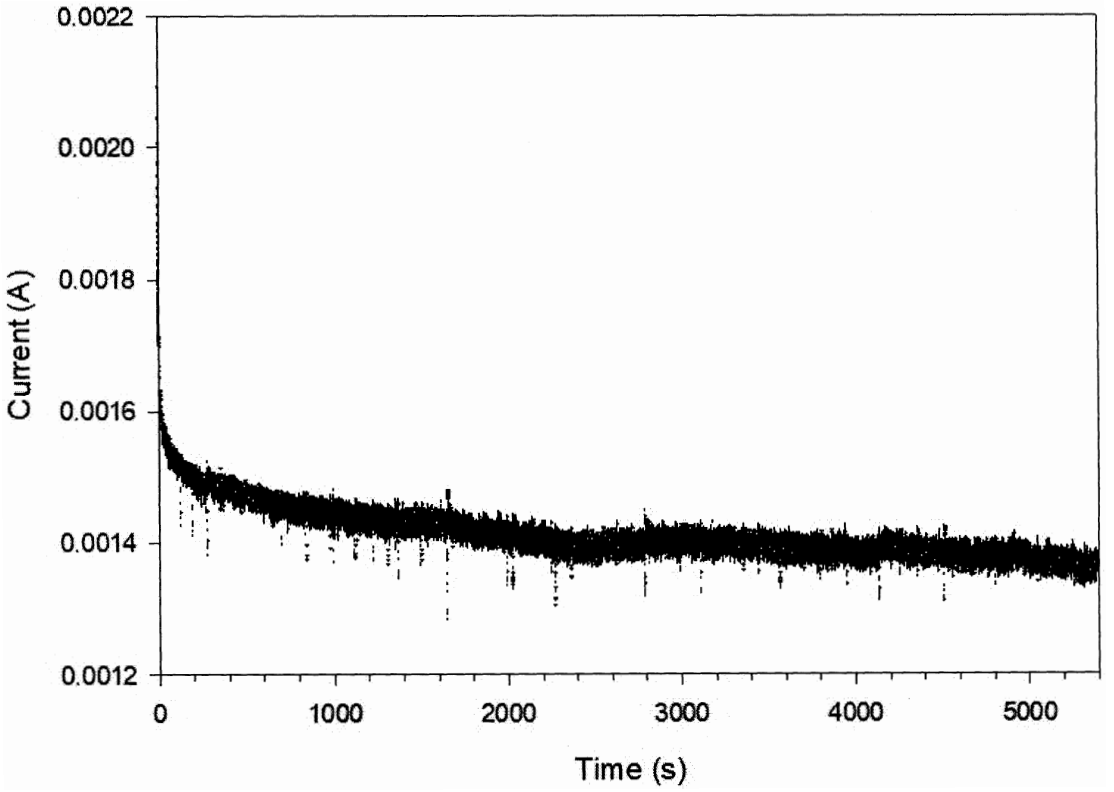

Figure 6. Amperommetric i-t curve of a 5 mm × 5 mm STO substrate (sample # 140709-02) with one contact at 1.2 V vs. Hg/HgO for 1.5 hours. The sensitivity level was 10^{-1} A/V.

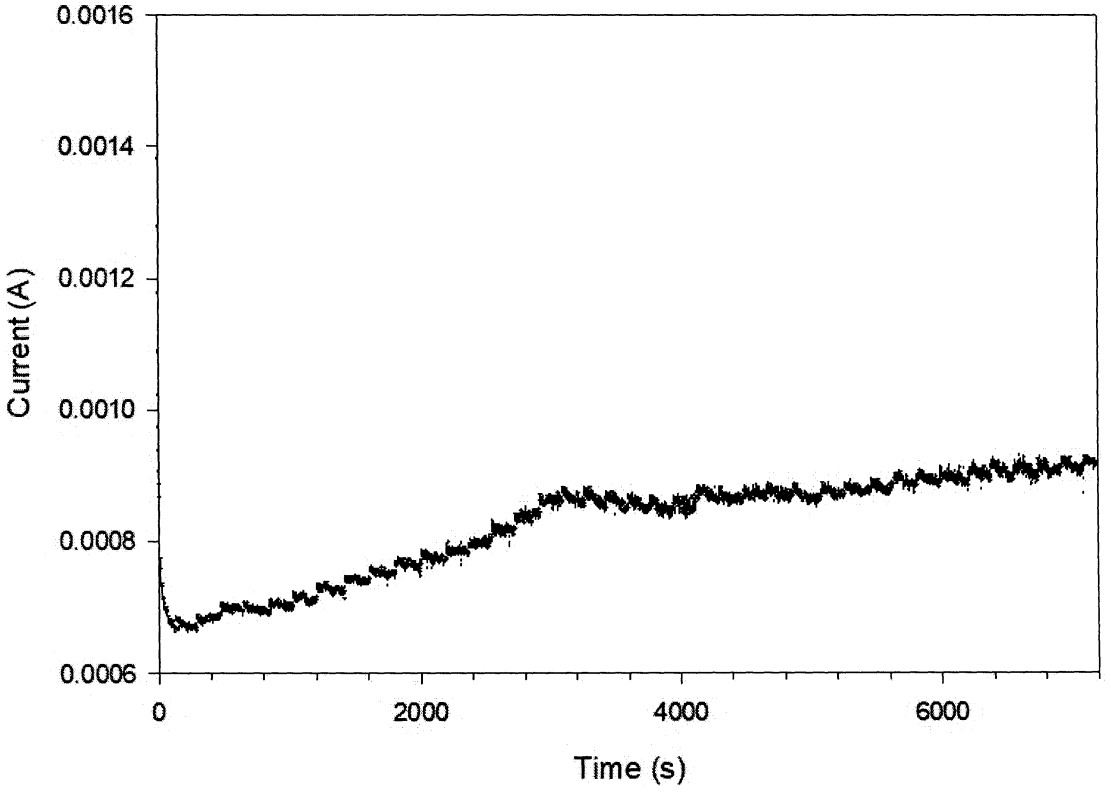

Figure 7. Amperommetric i-t curve of a 5 mm × 5 mm STO substrate (sample # 140710) with one contact at 1.2 V vs. Hg/HgO for 2 hours. The sensitivity level was 10^{-1} A/V.

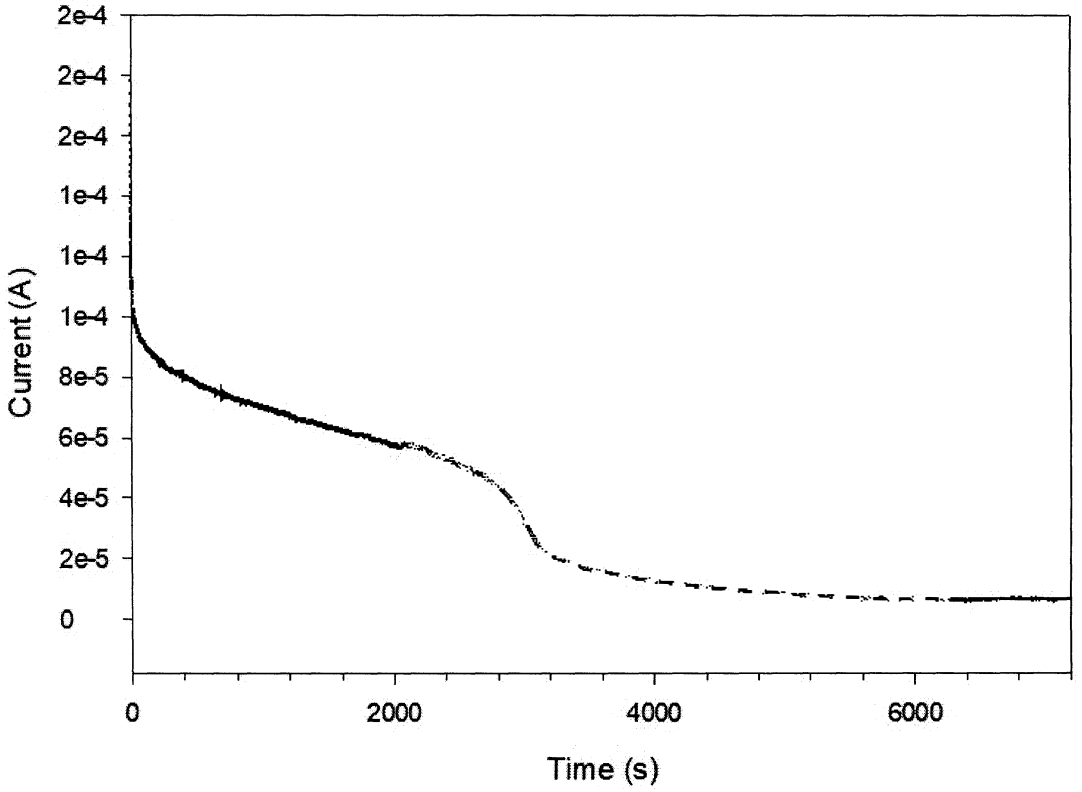

Figure 8. Amperommetric i-t curve of a 5 mm × 5 mm STO substrate (sample # 150807-01) with one contact at 0.8 V vs. Hg/HgO for 2 hours. The sensitivity level was 10^{-3} A/V.

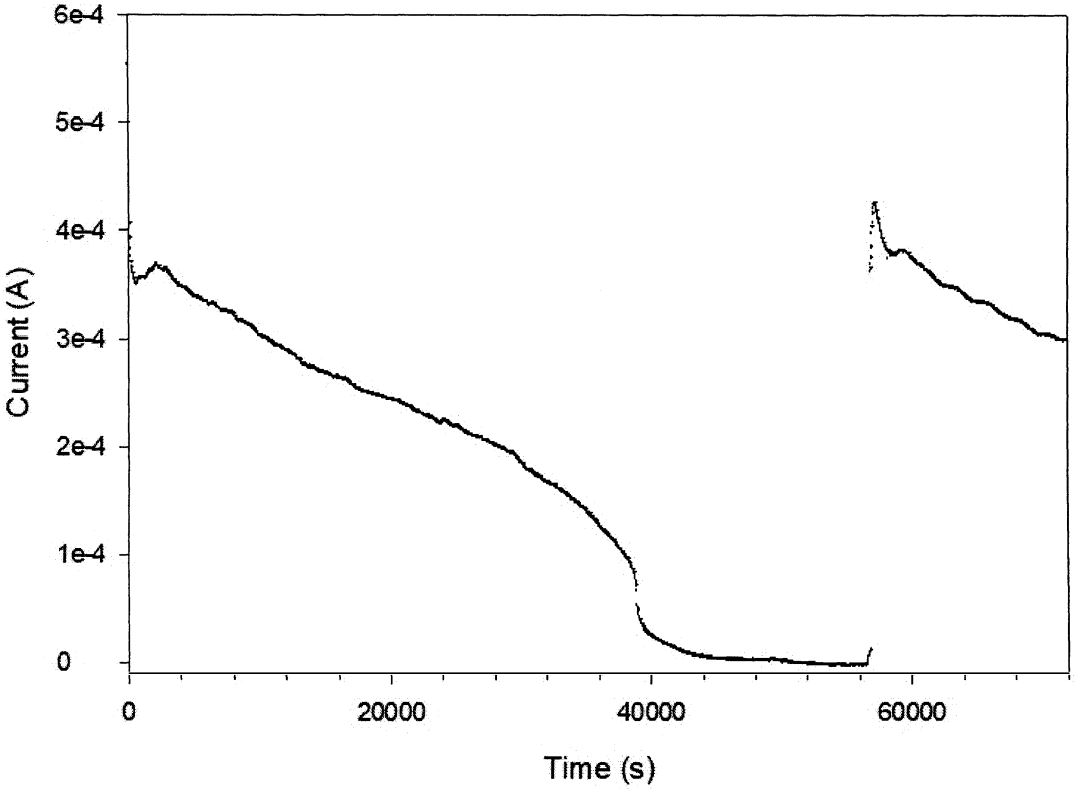

Figure 9. Amperommetric i-t curve of a 5 mm × 5 mm STO substrate (sample # 20160126) with one contact at 1.0 V vs. Hg/HgO for 20 hours. The sensitivity level was 10^{-3} A/V. Negative current values were observed between 51180 seconds (14.2 hours) and 56610 seconds (15.7 hours), and turned back to positive after a portion of electrolyte (1 M NaOH) was added to the cell to compensate for the amount evaporated during the 20 hours of the course of the experiment.

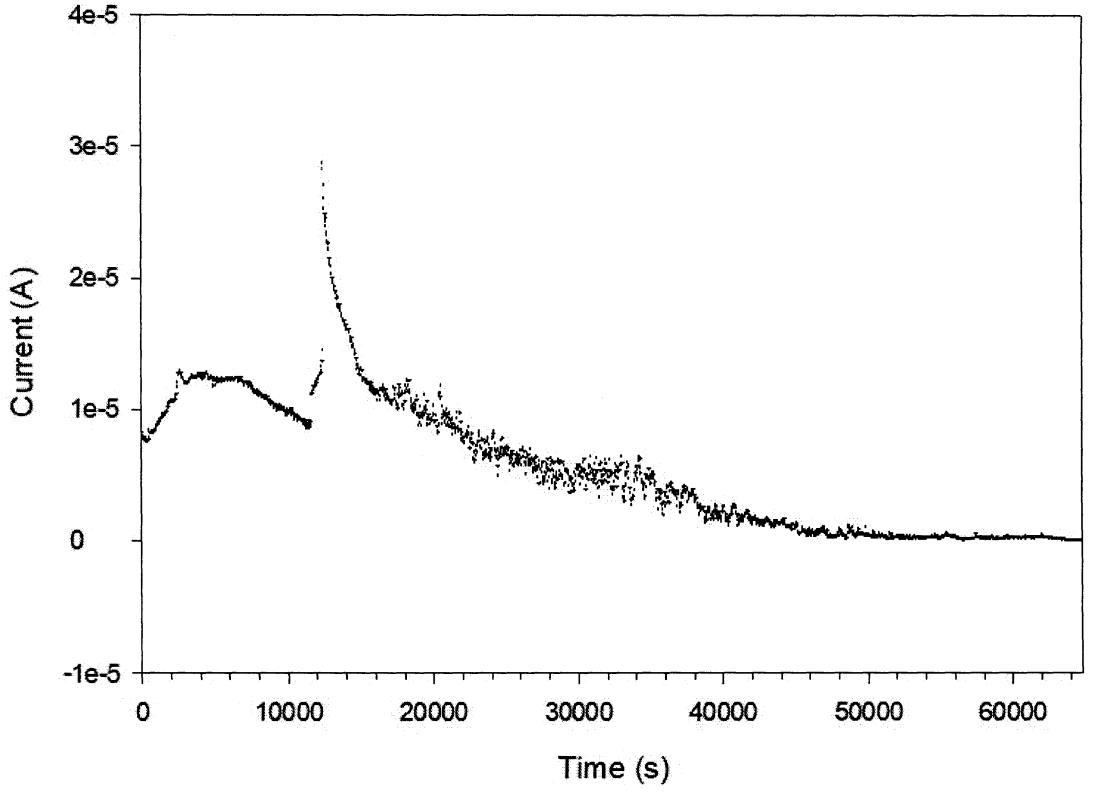

Figure 10. Amperommetric i-t curve of a 5 mm × 5 mm STO substrate (sample # 20160128) with one contact at 1.0 V vs. Hg/HgO for 18 hours. The sensitivity level was 10^{-3} A/V.

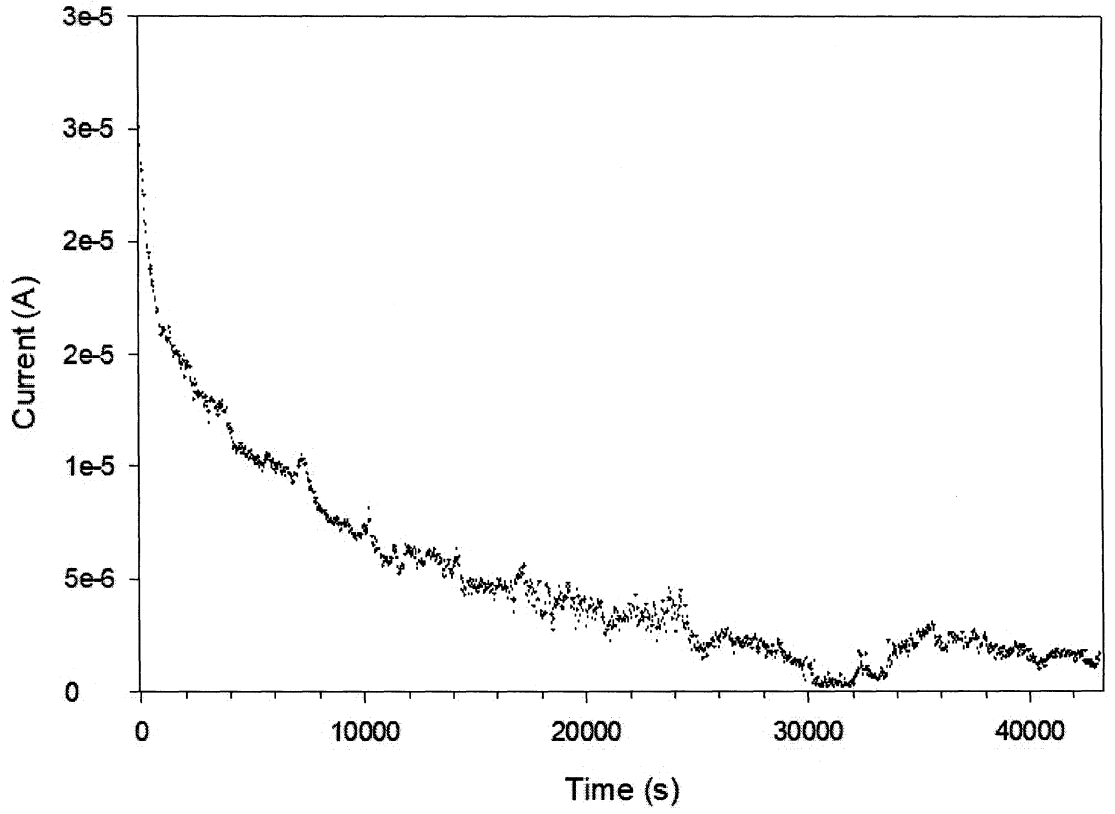

Figure 11. Amperommetric i-t curve of a 5 mm × 5 mm STO substrate (sample # 20160201) with one contact at 1.0 V vs. Hg/HgO for 12 hours. The sensitivity level was 10^{-5} A/V.

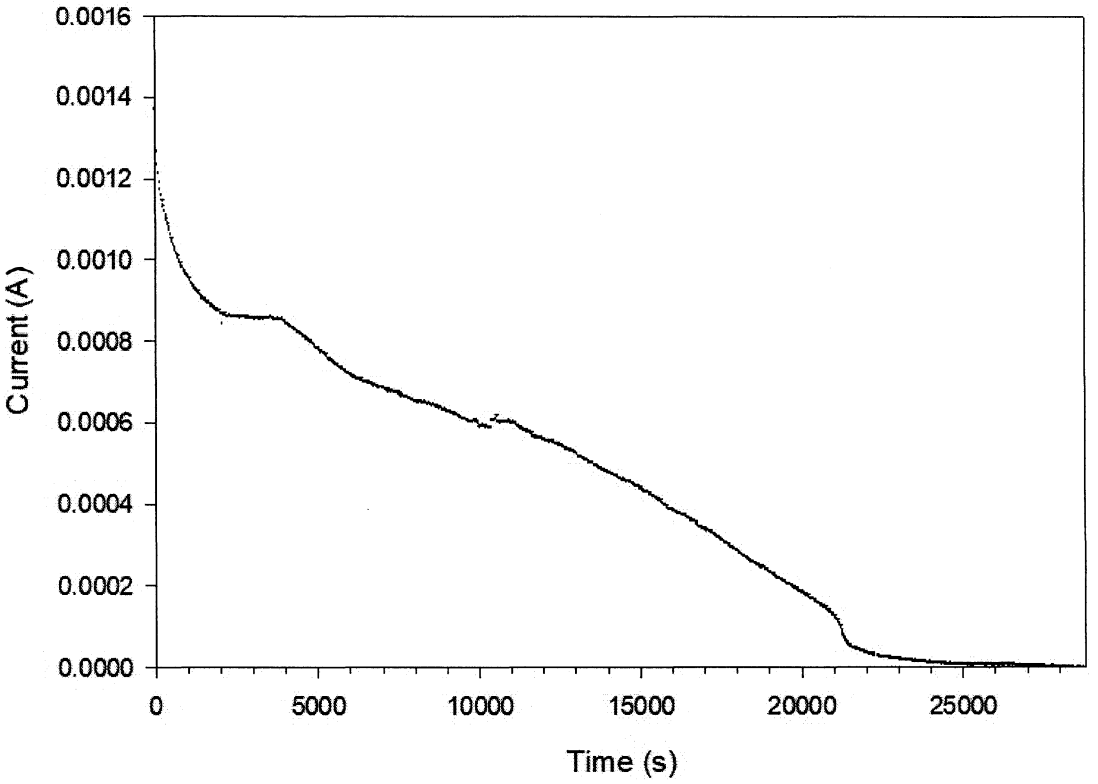

Figure 12. Amperommetric i-t curve of a 5 mm × 5 mm STO substrate (sample # 20160204) with one contact at 1.0 V vs. Hg/HgO for 8 hours and the sensitivity level was 10^{-3} A/V. Negative current values were recorded after ~28500 seconds.

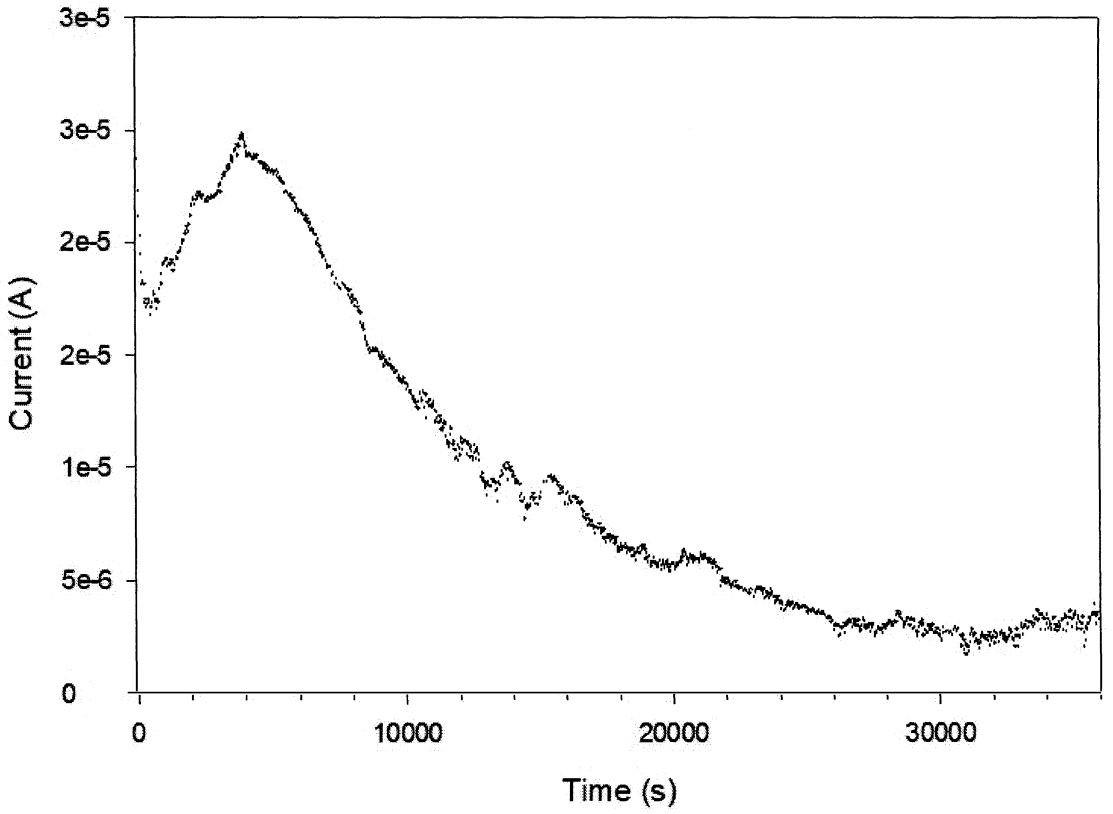

Figure 13. Amperommetric i-t curve of a 5 mm × 5 mm STO substrate (sample # 20160204, same substrate as Figure 12) with one contact at 1.0 V vs. Hg/HgO for another 10 hours after a portion of 1 M NaOH electrolyte was added to compensate for the evaporated electrolyte. Sensitivity level was set to 10^{-5} A/V.

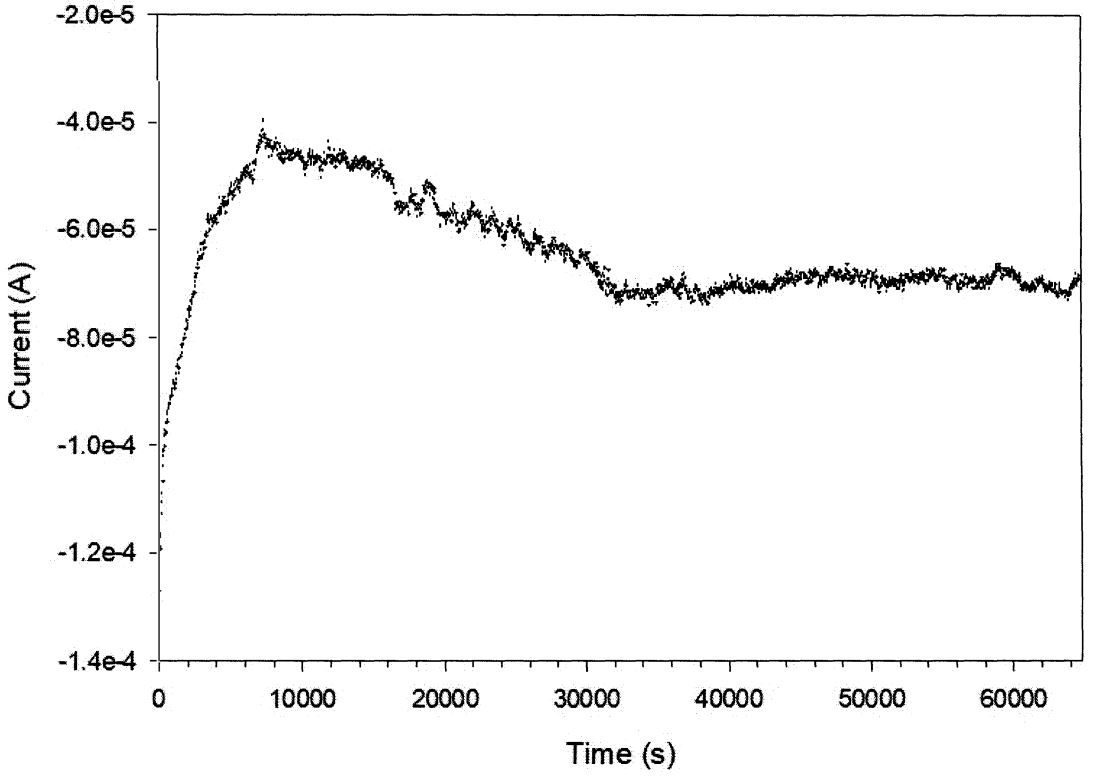

Figure 14. Amperommetric i-t curve of a 10 mm × 10 mm STO substrate (sample # 140918) with one contacts at 1.7 V vs. Hg/HgO for 18 hours. The sensitivity was 10^{-1} A/V.

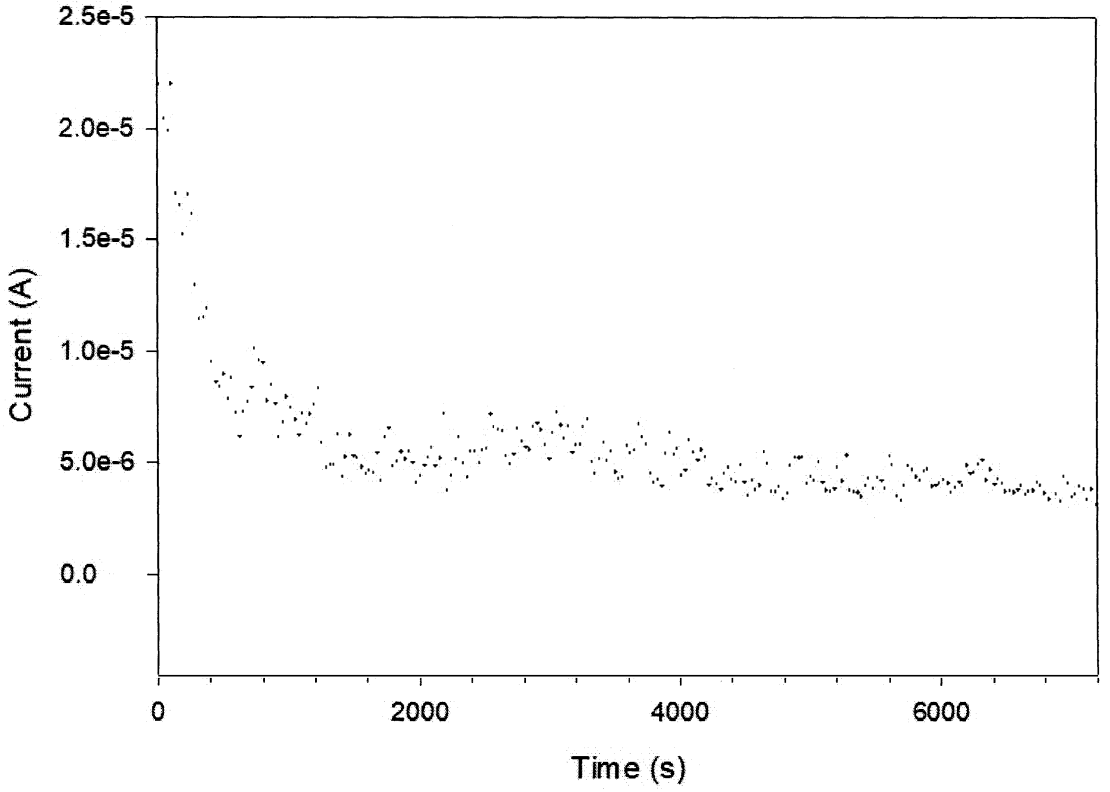

Figure 15. Amperommetric i-t curve of a 10 mm × 10 mm STO substrate (sample # 140924) with one contact at 1.7 V vs. Hg/HgO for 2 hours. The sensitivity was 10^{-4} A/V.

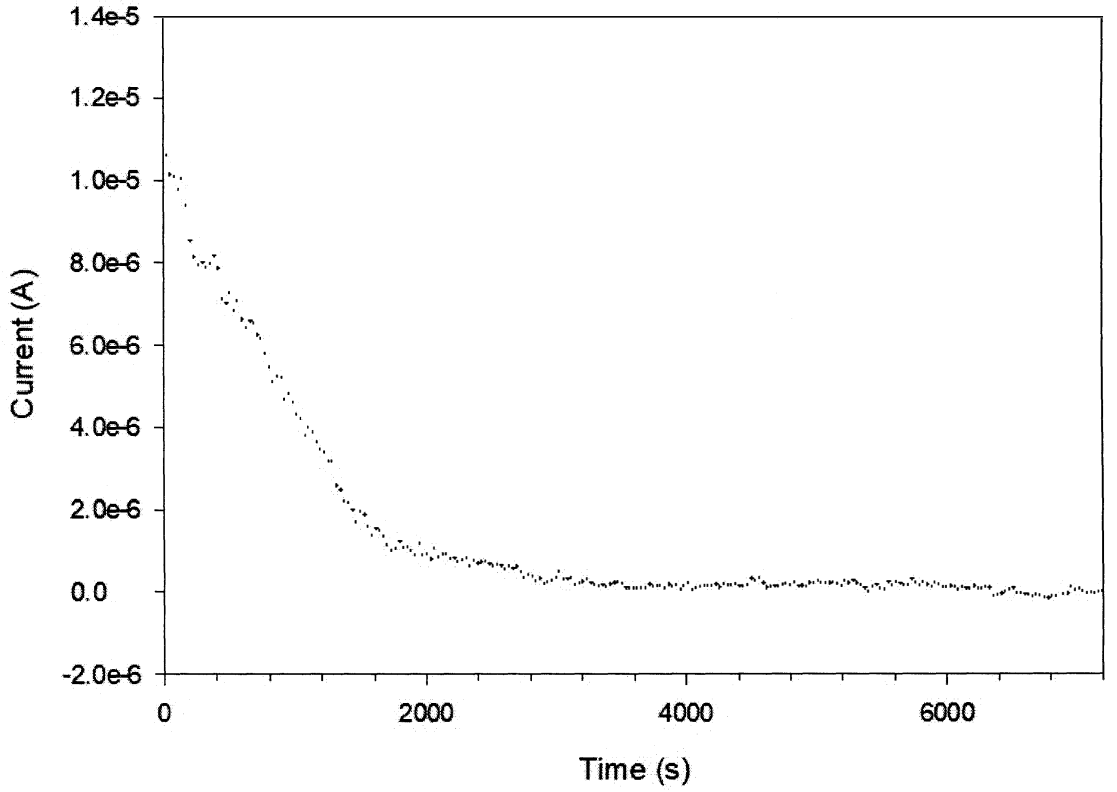

Figure 16. Amperommetric i-t curve of a 10 mm × 10 mm STO substrate (sample # 141001-01) with one contact at 1.7 V vs. Hg/HgO for 2 hours. The sensitivity was 10^{-4} A/V.

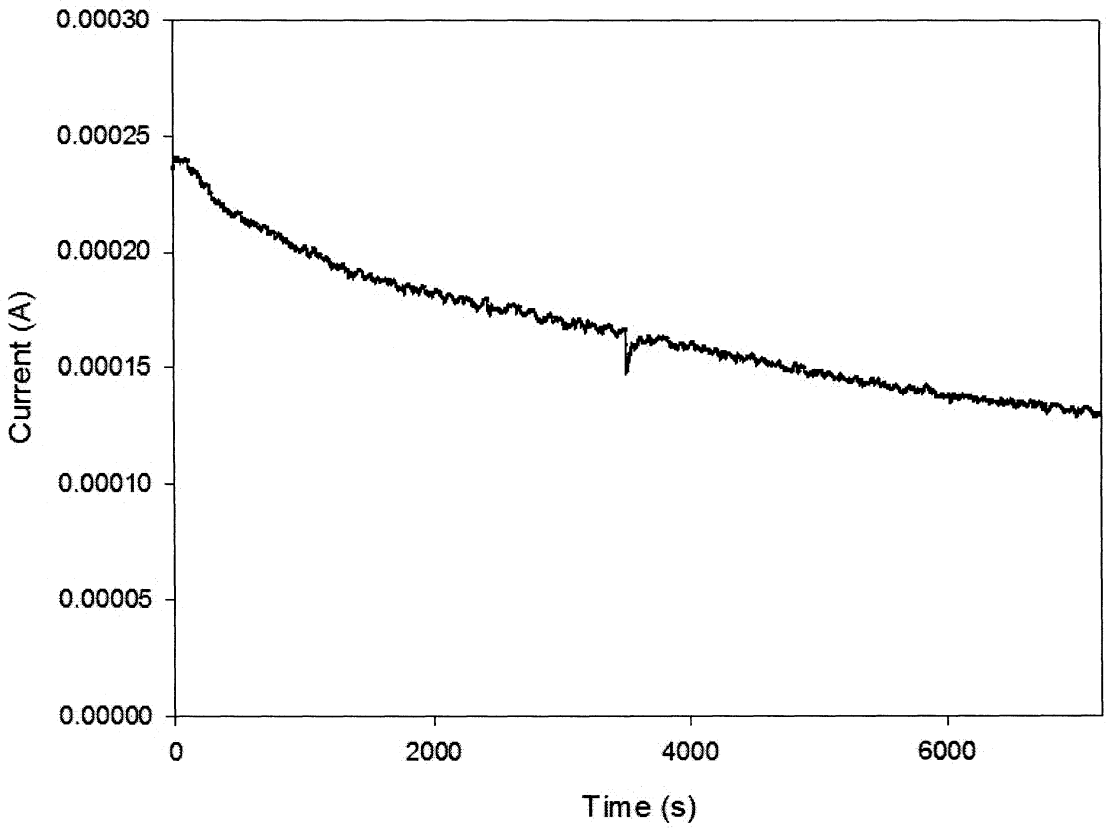

Figure 17. Amperommetric i-t curve of a 10 mm × 10 mm STO substrate (sample # 141010-01) with one contact at 1.7 V vs. Hg/HgO for 2 hours. The sensitivity was 10^{-2} A/V.

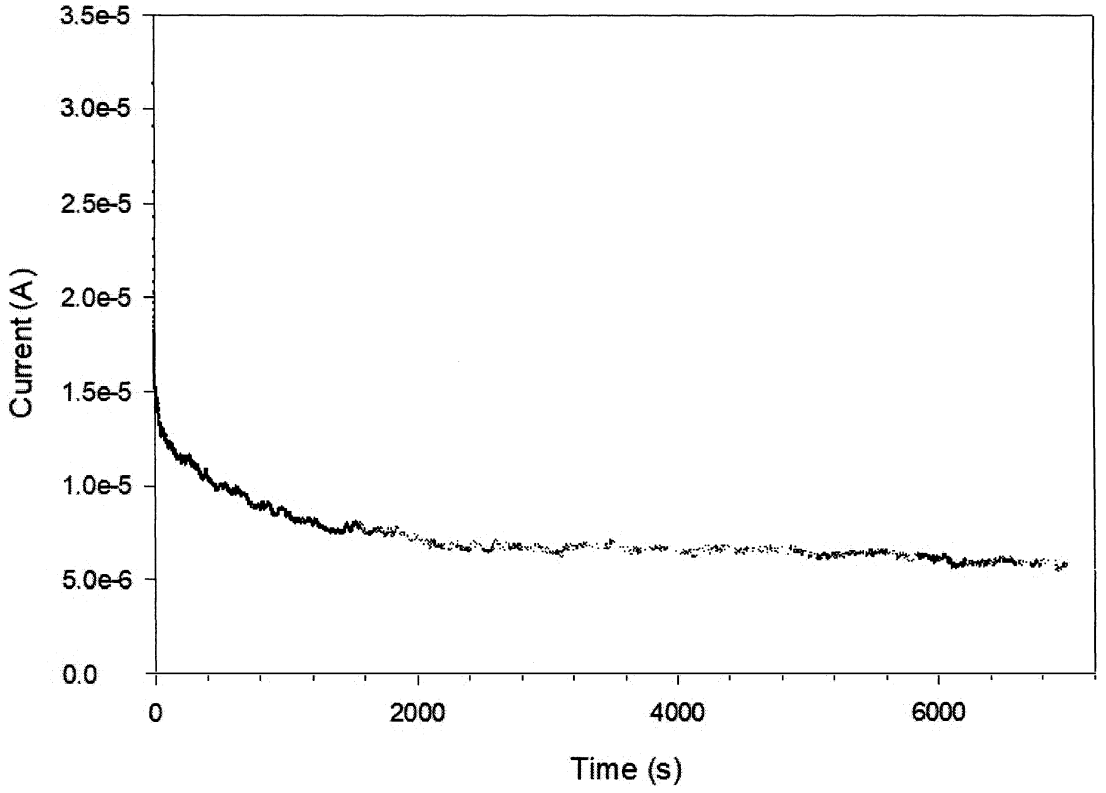

Figure 18. Amperommetric i-t curve of a 10 mm × 10 mm STO substrate (sample # 141103-1) with one contact at 1.0 V vs. Hg/HgO for 2 hours. The sensitivity was 10^{-4} A/V.

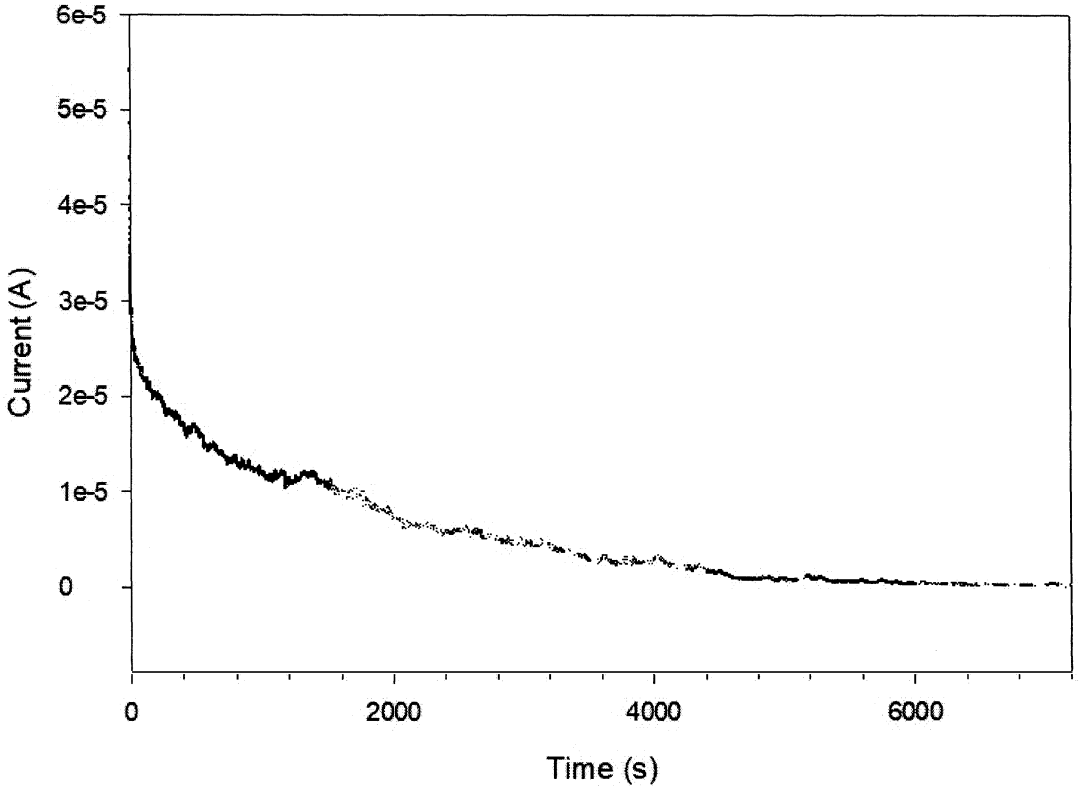

Figure 19. Amperommetric i-t curve of a 10 mm × 10 mm STO substrate (sample # 141212) with one contact at 1.0 V vs. Hg/HgO for 2 hours. The sensitivity was 10^{-4} A/V.

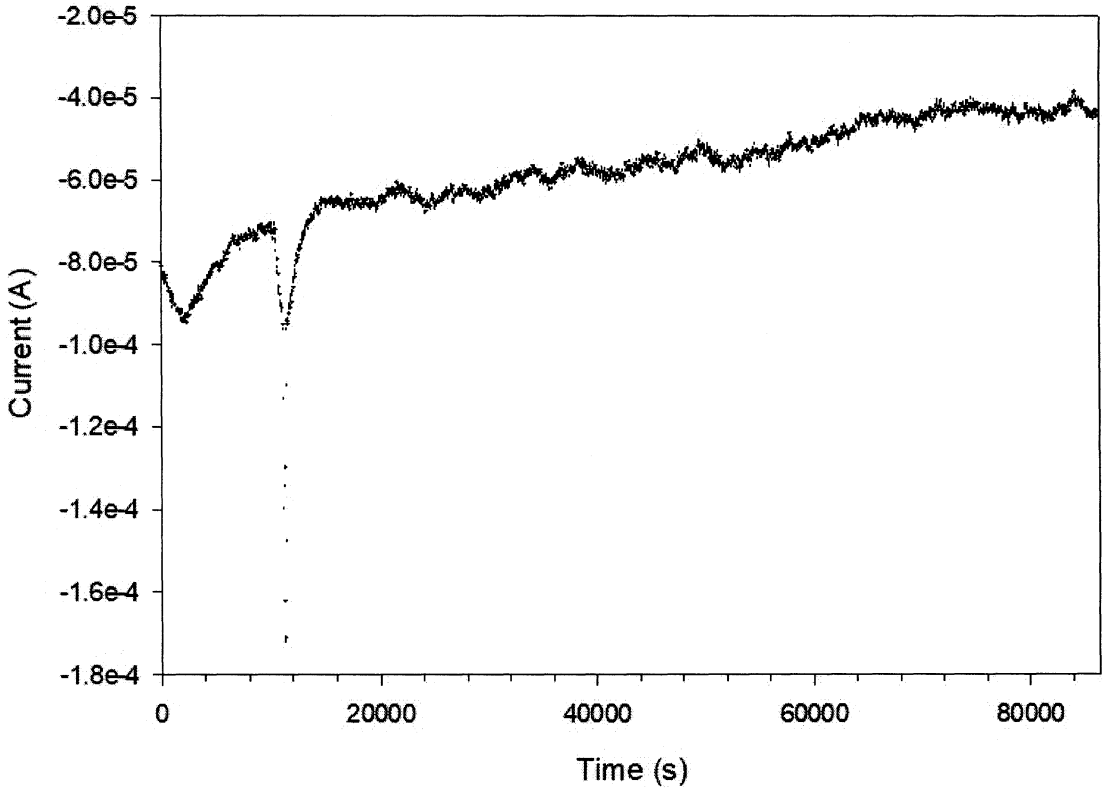

Figure 20. Amperommetric i-t curve of a 10 mm × 10 mm STO substrate (sample # 140703） with two contacts at 1.2 V vs. Hg/HgO for 24 hours as the first electrochemical modification. The sensitivity was 10^{-1} A/V.

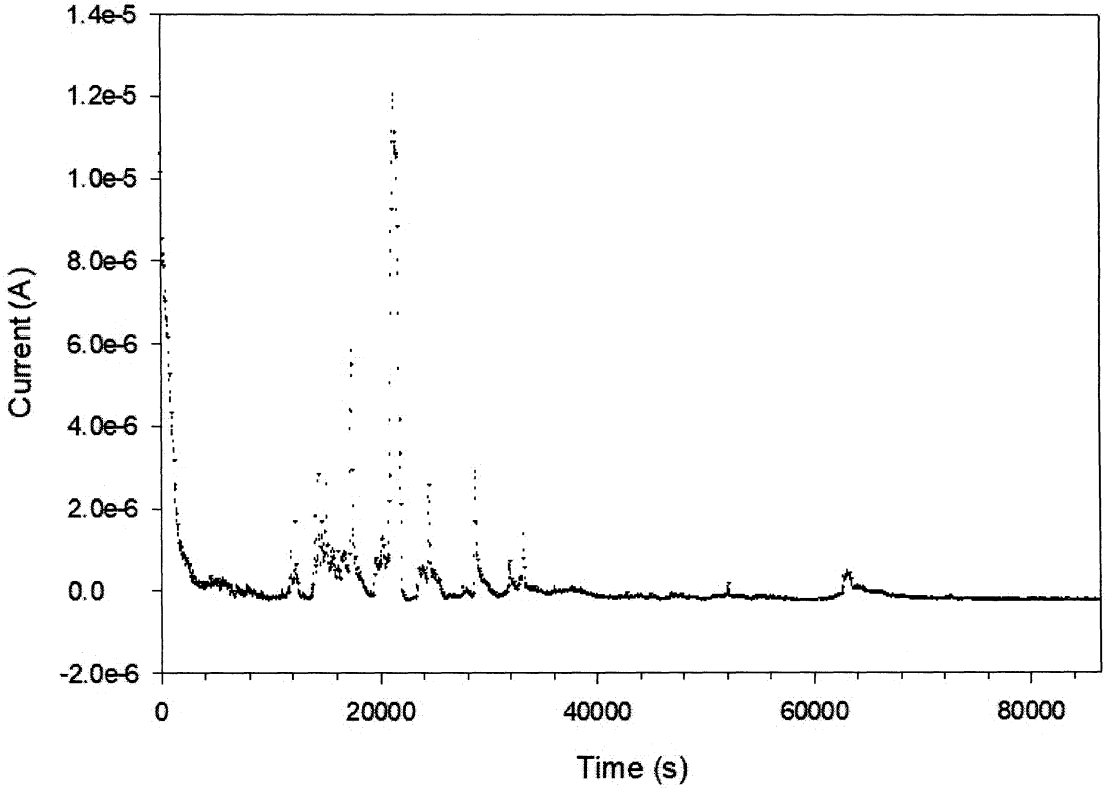

Figure 21. Amperommetric i-t curve of a 10 mm × 10 mm STO substrate (sample # 140703, same substrate as Figure 4a) with two contacts at 1.2 V vs. Hg/HgO for 24 hours as the second electrochemical modification. The sensitivity was 10^{-4} A/V.

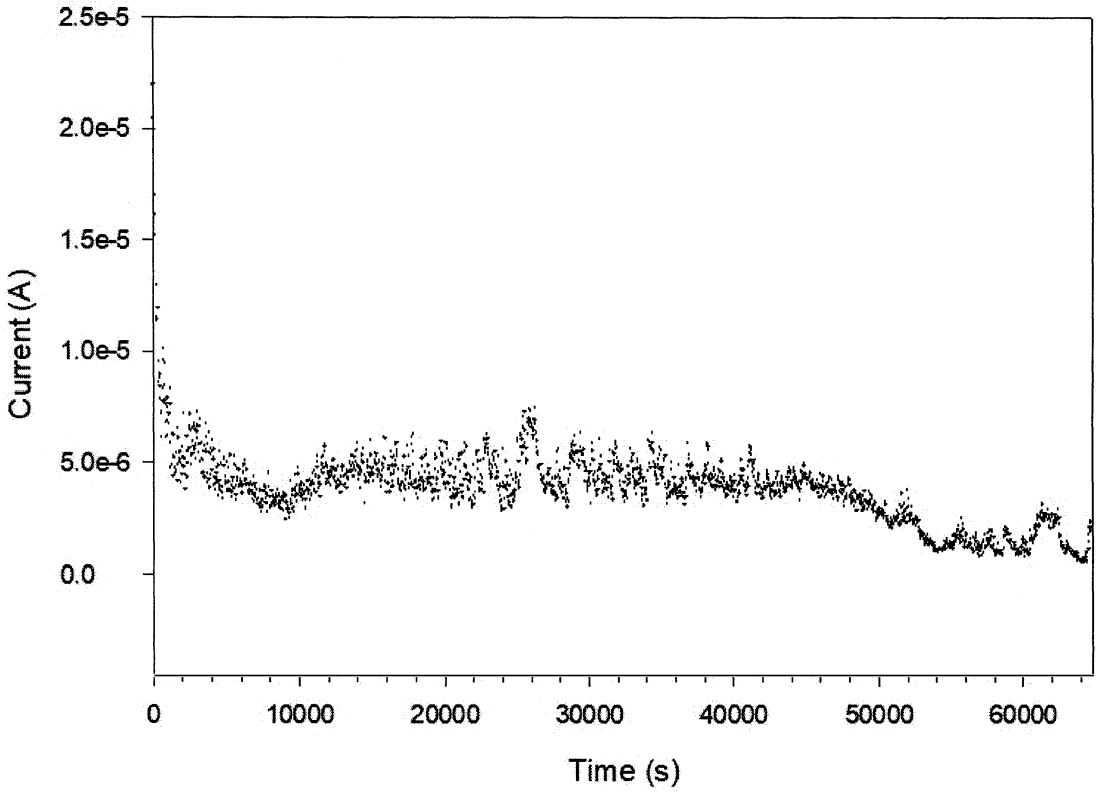

Figure 22. Amperommetric i-t curve of a 10 mm × 10 mm STO substrate (sample # 140829-01) with two contacts at 1.7 V vs. Hg/HgO for 18 hours. The sensitivity was 10^{-4} A/V.

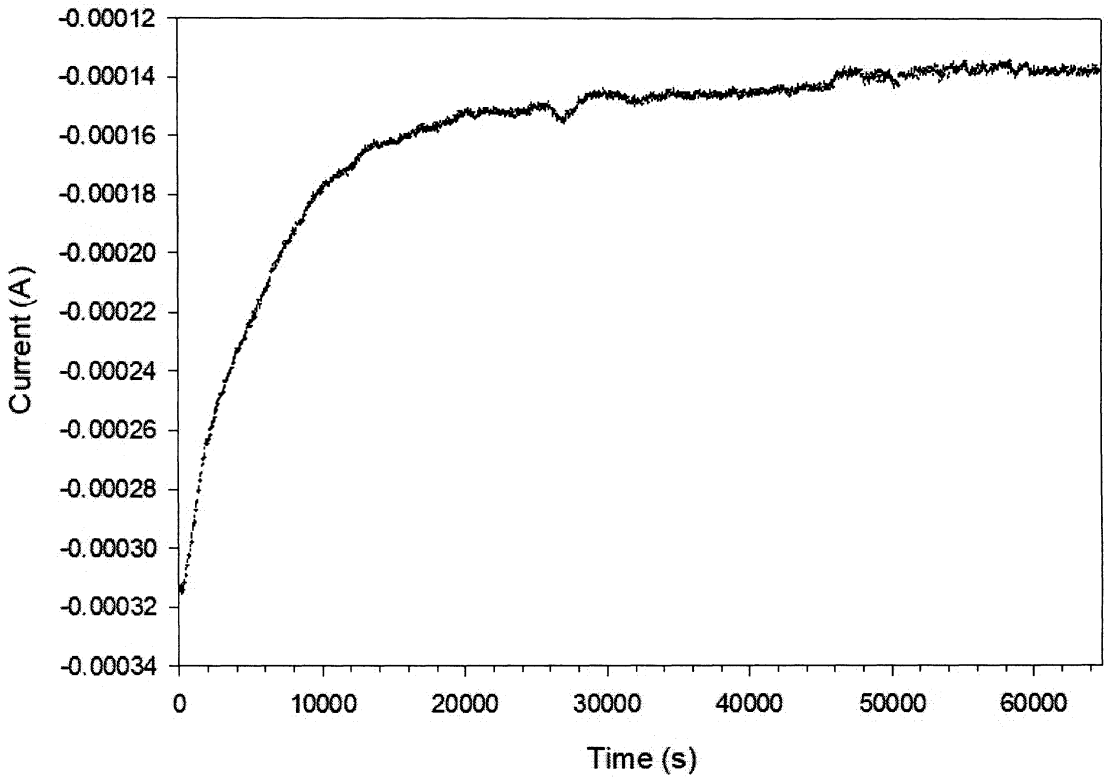

Figure 23. Amperommetric i-t curve of a 10 mm × 10 mm STO substrate (sample # 20140903-01) with two contacts at 1.7 V vs. Hg/HgO for 18 hours. The sensitivity was 10^{-1} A/V.

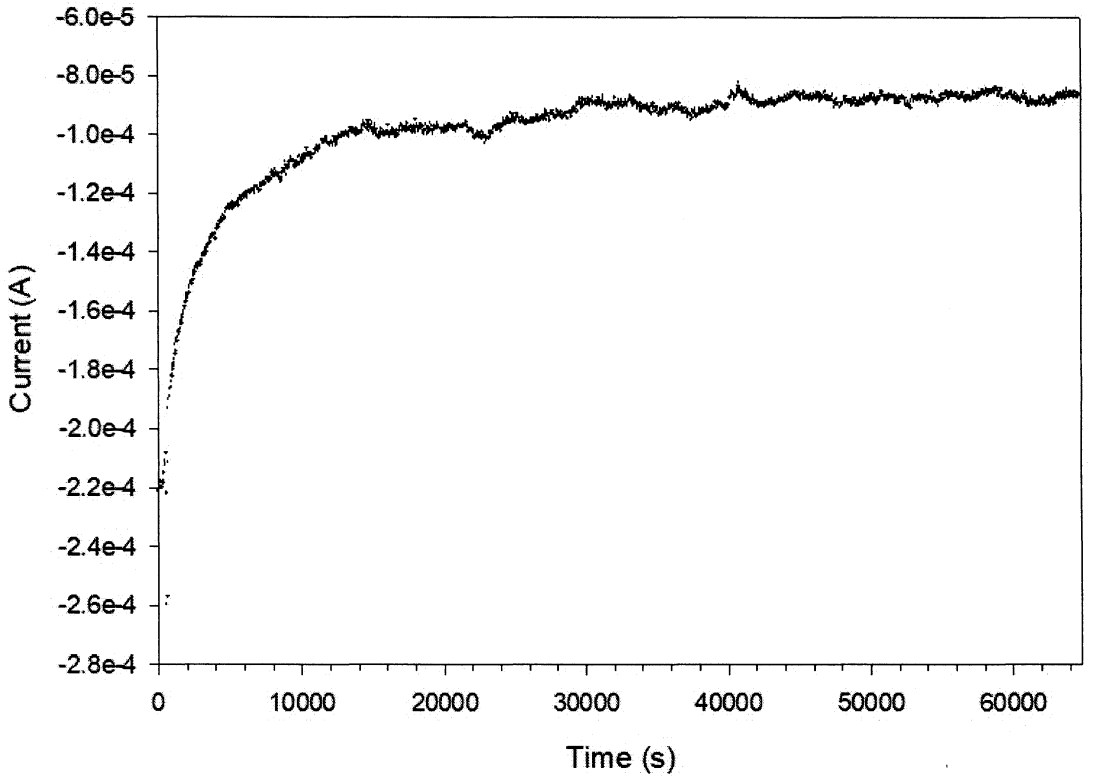

Figure 24. Amperommetric i-t curve of a 10 mm × 10 mm STO substrate (sample # 20140908-01) with two contacts at 1.7 V vs. Hg/HgO for 18 hours. The sensitivity was 10^{-1} A/V.

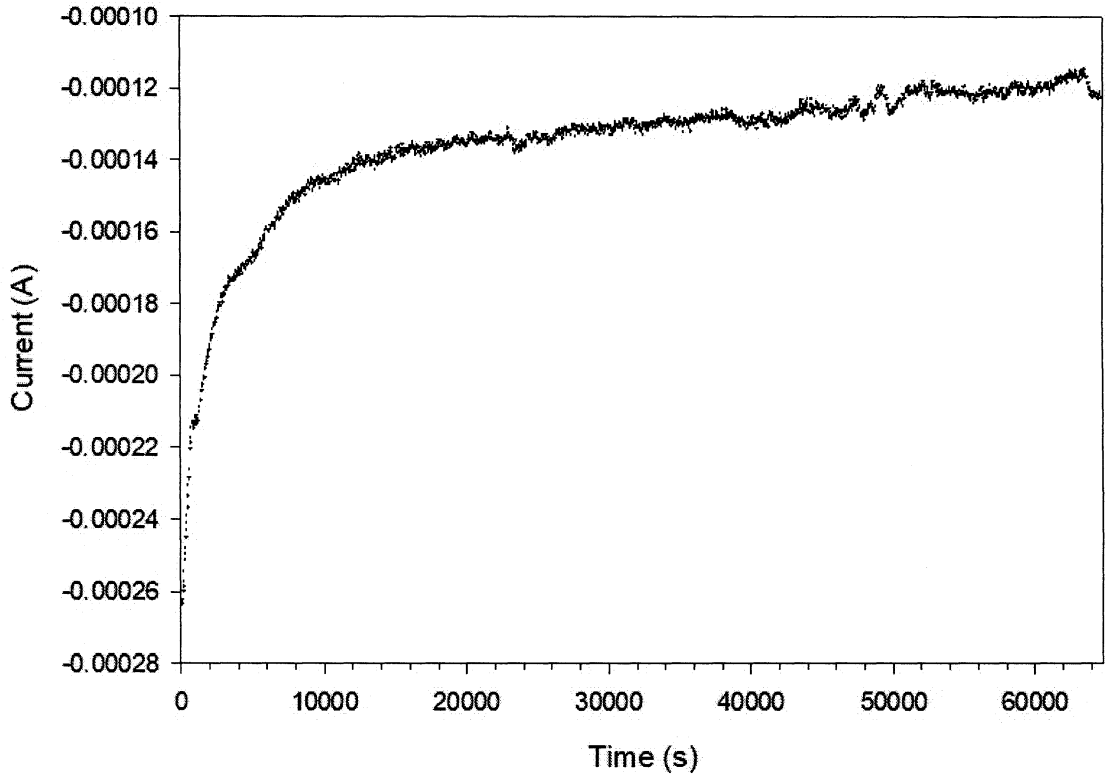

Figure 25. Amperommetric i-t curve of a 10 mm × 10 mm STO substrate (sample # 20140909-01) with two contacts at 1.7 V vs. Hg/HgO for 18 hours. The sensitivity was 10^{-1} A/V.

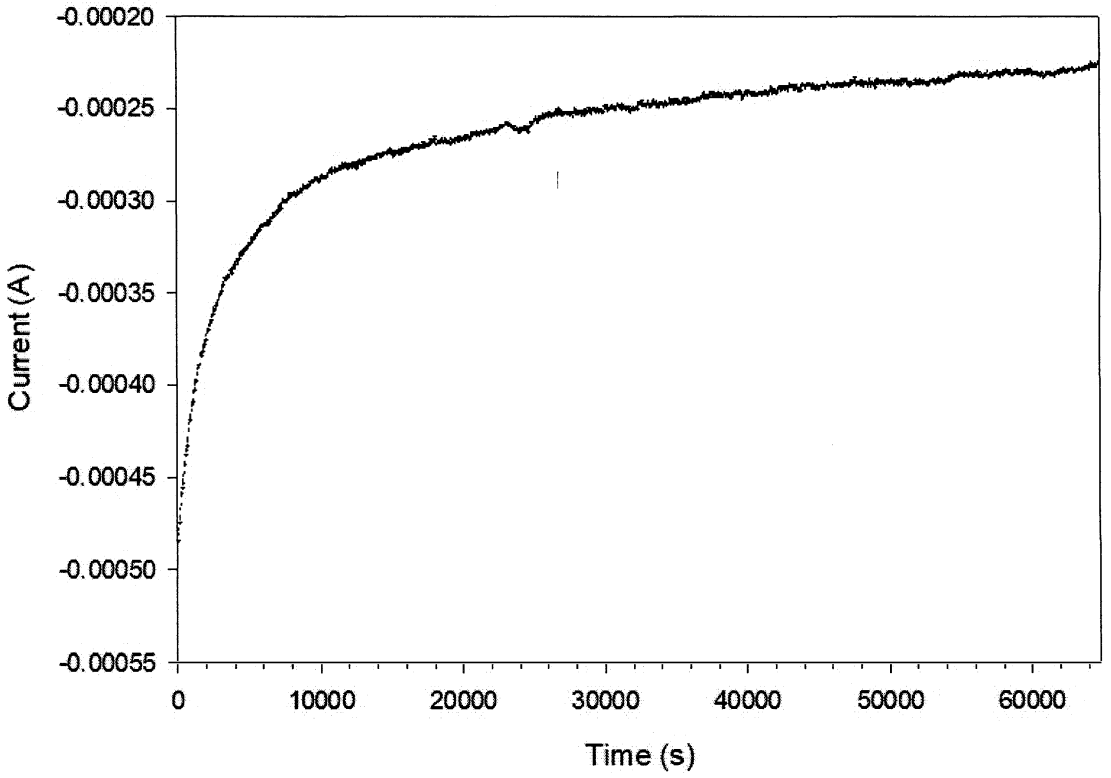

Figure 26. Amperommetric i-t curve of a 10 mm × 10 mm STO substrate (sample # 20140916-01) with two contacts at 1.7 V vs. Hg/HgO for 18 hours. The sensitivity was 10^{-1} A/V.

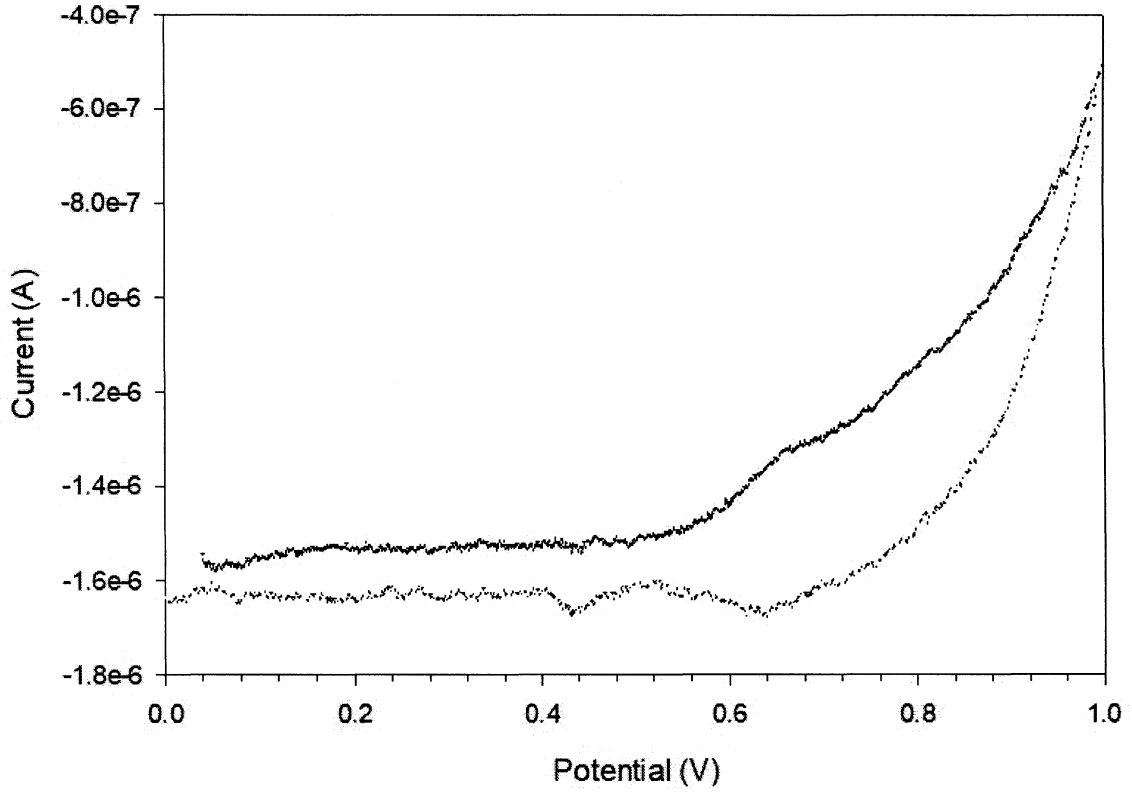

Figure 27. Cyclic voltammogram of a 10 mm × 10 mm $SrTiO_3$ substrate (sample # 141202-01) with one contact (scan rate: 0.01 V/s; RE: Hg/HgO). The sensitivity was 10^{-3} A/V.

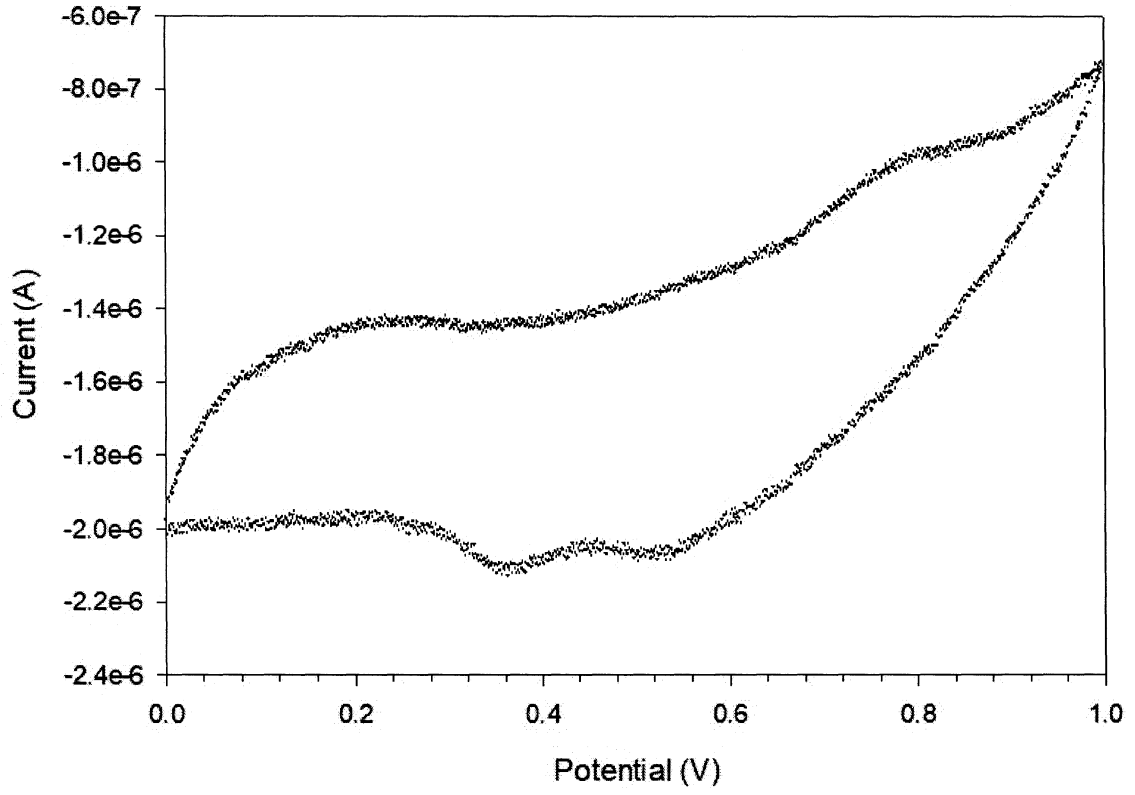

Figure 28. Cyclic voltammogram of a 10 mm × 10 mm $SrTiO_3$ substrate (sample # 141203-01) with one contact (scan rate: 0.1 V/s; RE: Hg/HgO). The sensitivity was 10^{-3} A/V.

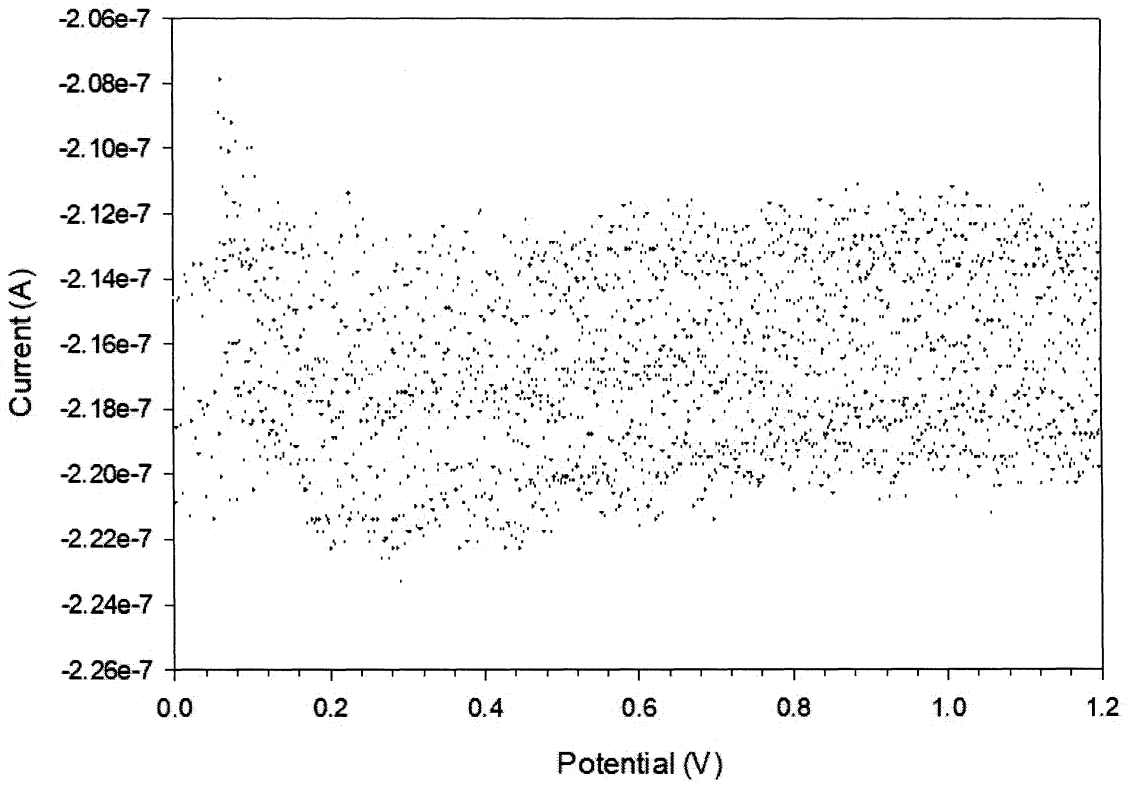

Figure 29. Cyclic voltammogram of a 10 mm × 10 mm $SrTiO_3$ substrate (sample # 141216-01) with two contacts (scan rate: 0.1 V/s; RE: Hg/HgO). The sensitivity was 10^{-4} A/V.

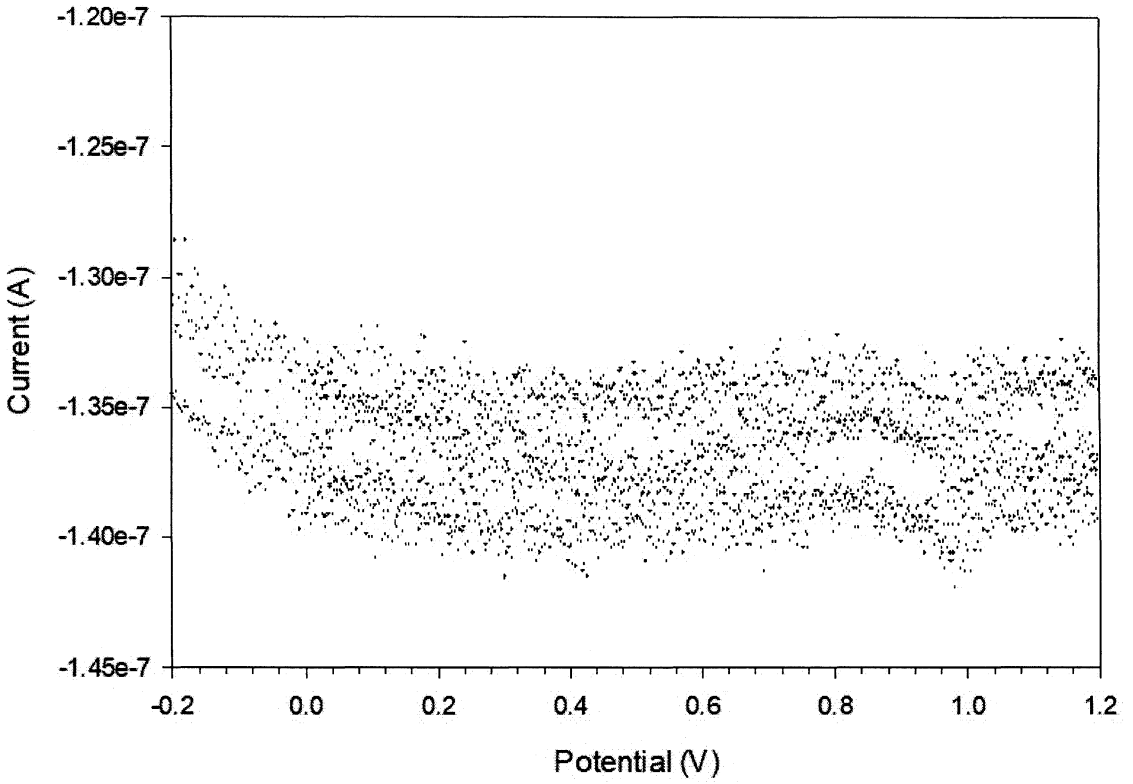

Figure 30. Cyclic voltammogram of a 10 mm × 10 mm $SrTiO_3$ substrate (sample # 141216-01, same substrate as Figure 4c) with one contact (scan rate: 0.01 V/s; RE: Hg/HgO). The sensitivity was 10^{-4} A/V.

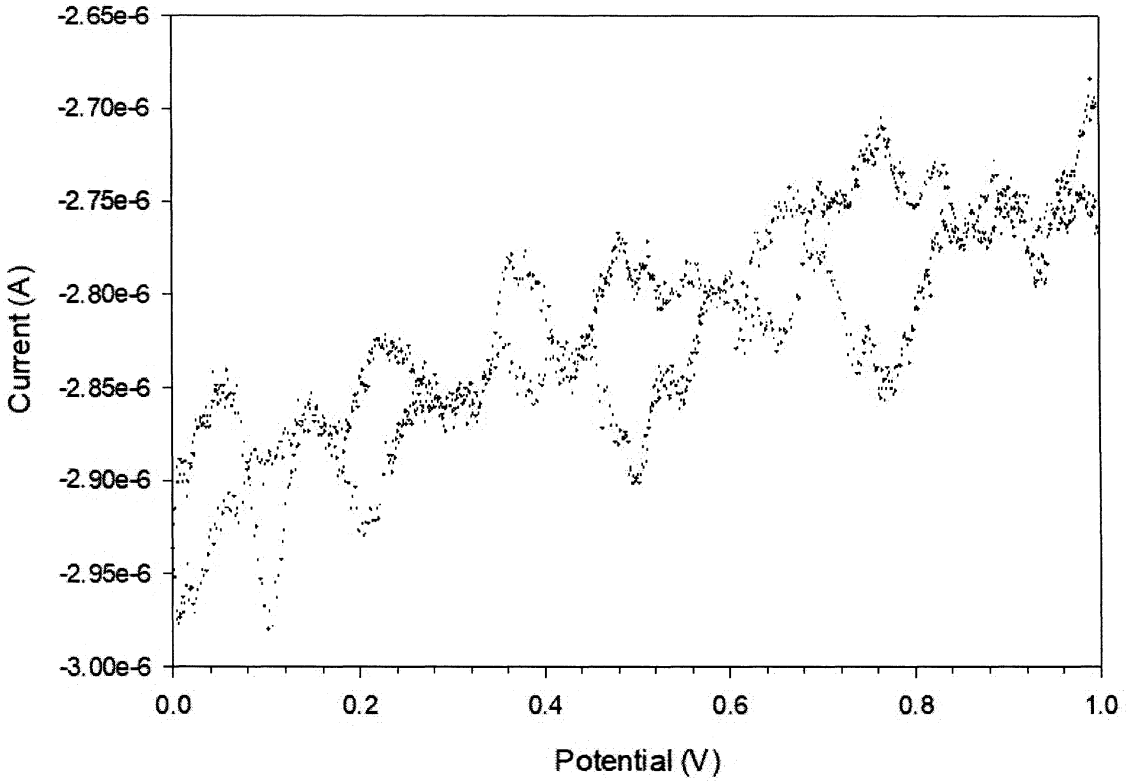

Figure 31. Cyclic voltammogram of a 10 mm × 10 mm $SrTiO_3$ substrate (sample # 150808-01) with one contact (scan rate: 0.05 V/s; RE: Hg/HgO). The sensitivity was 10^{-3} A/V.

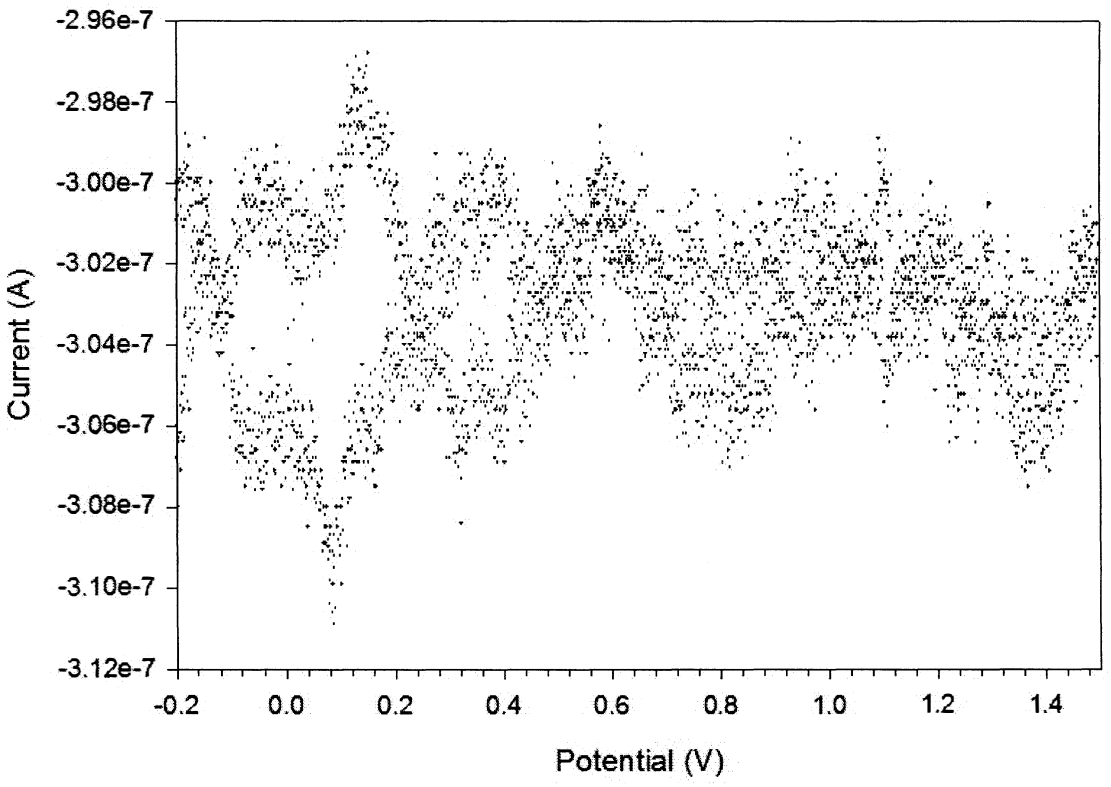

Figure 32. Cyclic voltammogram of a 10 mm × 10 mm $SrTiO_3$ substrate (sample # 140703) with two contacts (scan rate: 0.1 V/s; RE: Hg/HgO). The sensitivity was 10^{-4} A/V. This voltammogram was taken after the potentiostatic treatment.

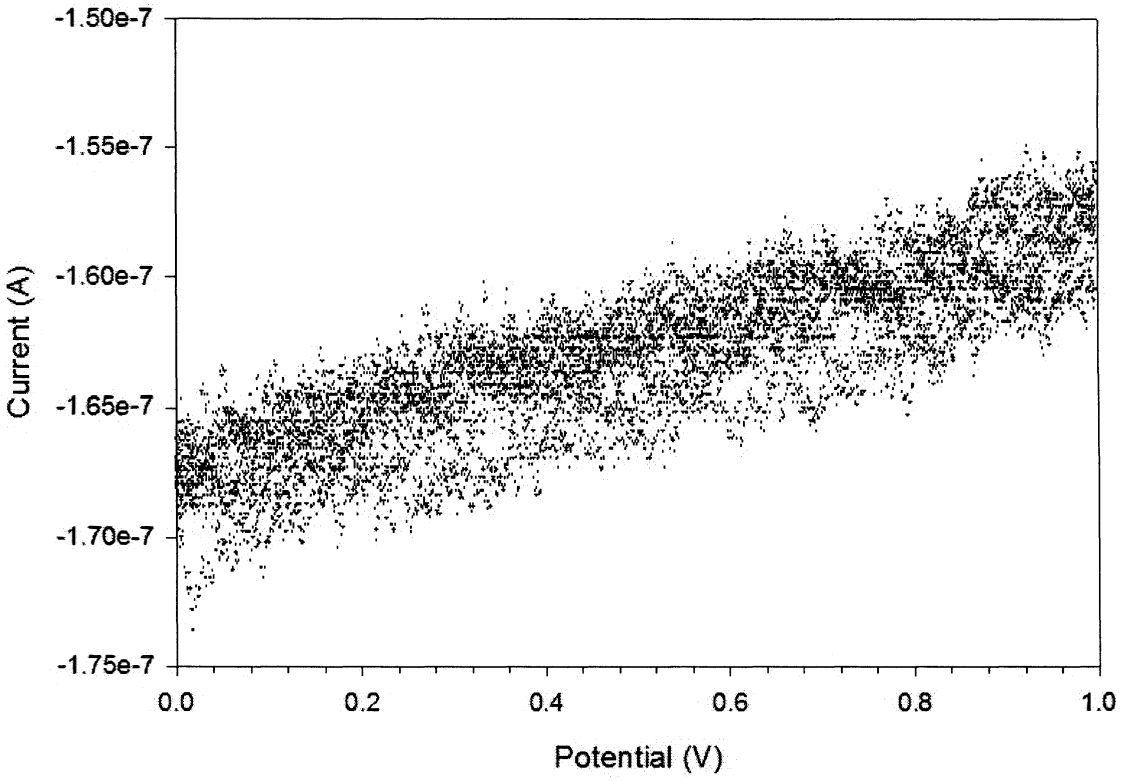

Figure 33. g) Cyclic voltammogram of a 10 mm × 10 mm $SrTiO_3$ substrate (sample # 20140916-01) with two contacts (scan rate: 0.01 V/s; RE: Hg/HgO). The sensitivity was 10^{-4} A/V.

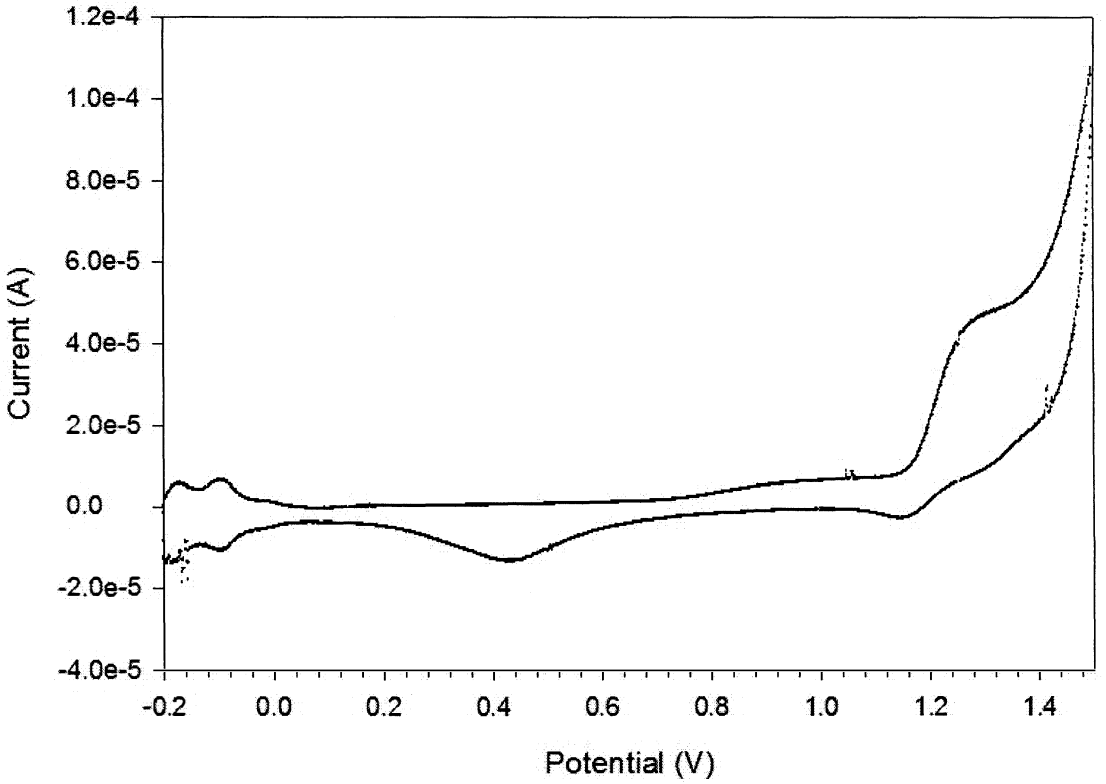

Figure 34. Cyclic voltammogram of a Pt wire in 0.5 M H_2SO_4 (scan rate: 0.1 V/s; RE: Ag/AgCl). The sensitivity was 10^{-4} A/V.

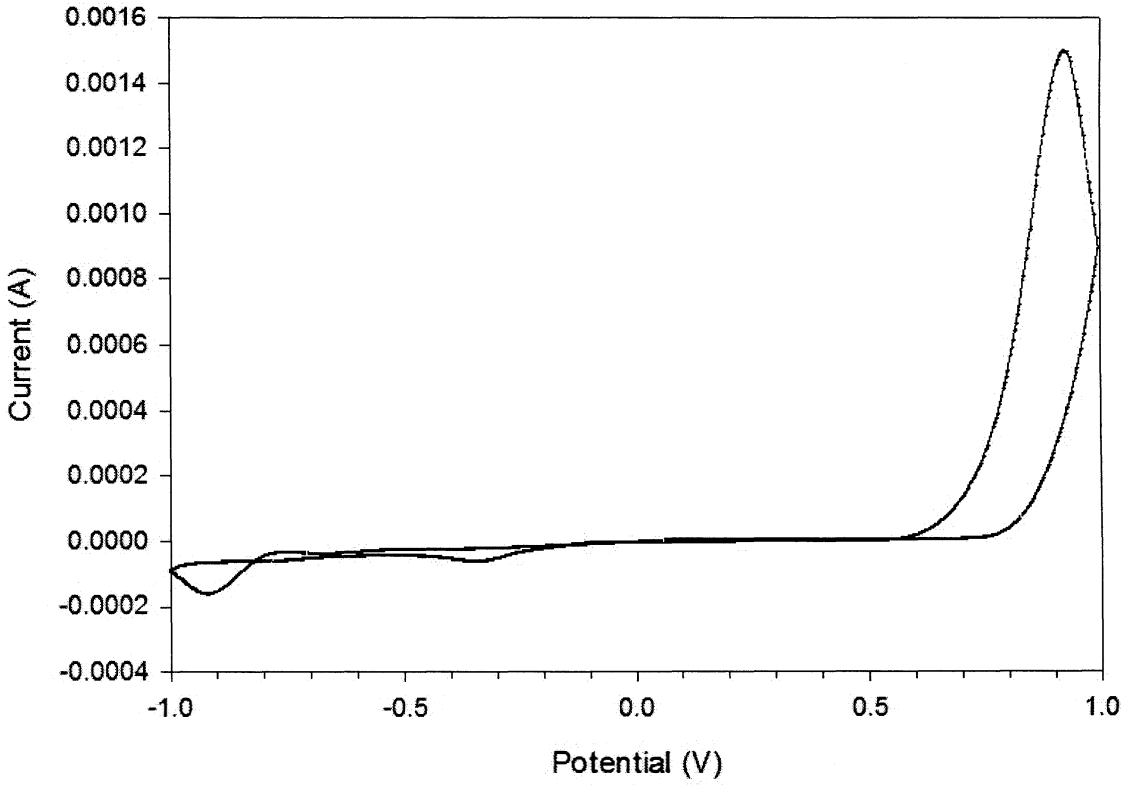

Figure 35. Cyclic voltammogram of a Pt wire in 1 M NaOH (scan rate: 0.05 V/s; RE: Hg/HgO). The sensitivity was 10^{-3} A/V.

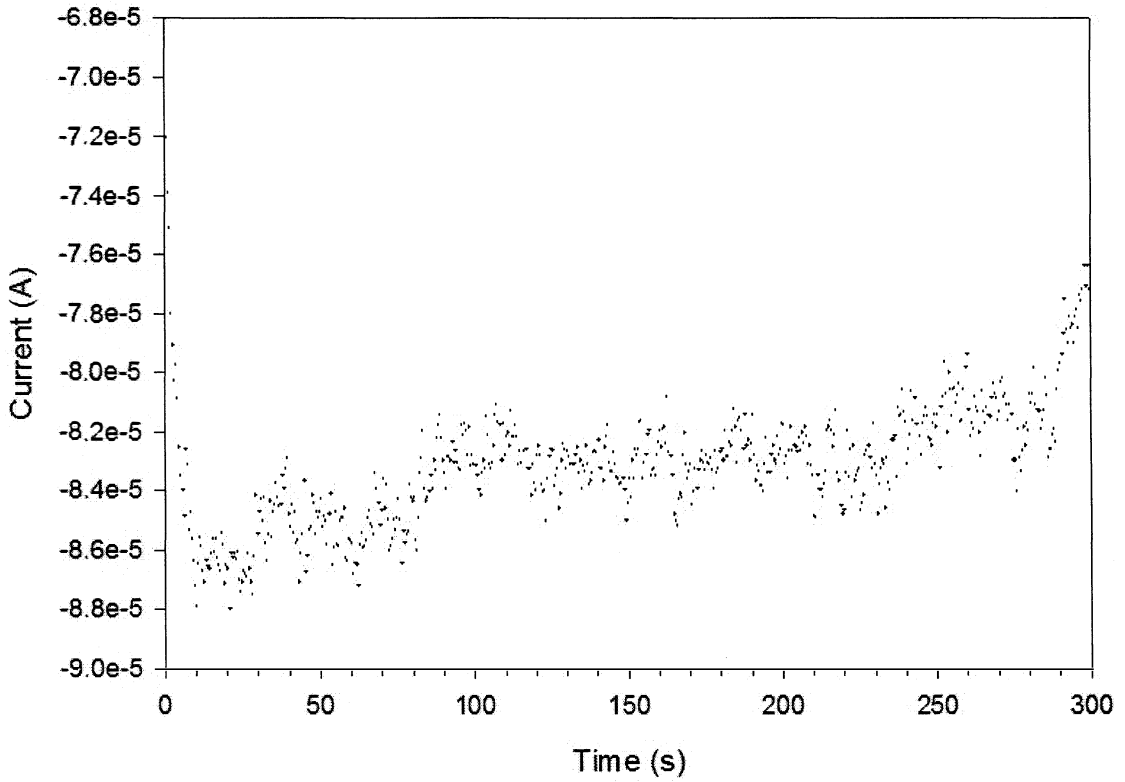

Figure 36. Amperometric i-t curve of a 10 mm × 10 mm $SrTiO_3$ substrate (sample # 140924) with two contacts at 1.7 V vs Ag/AgCl for 5 minutes. The sensitivity was 10^{-1} A/V.

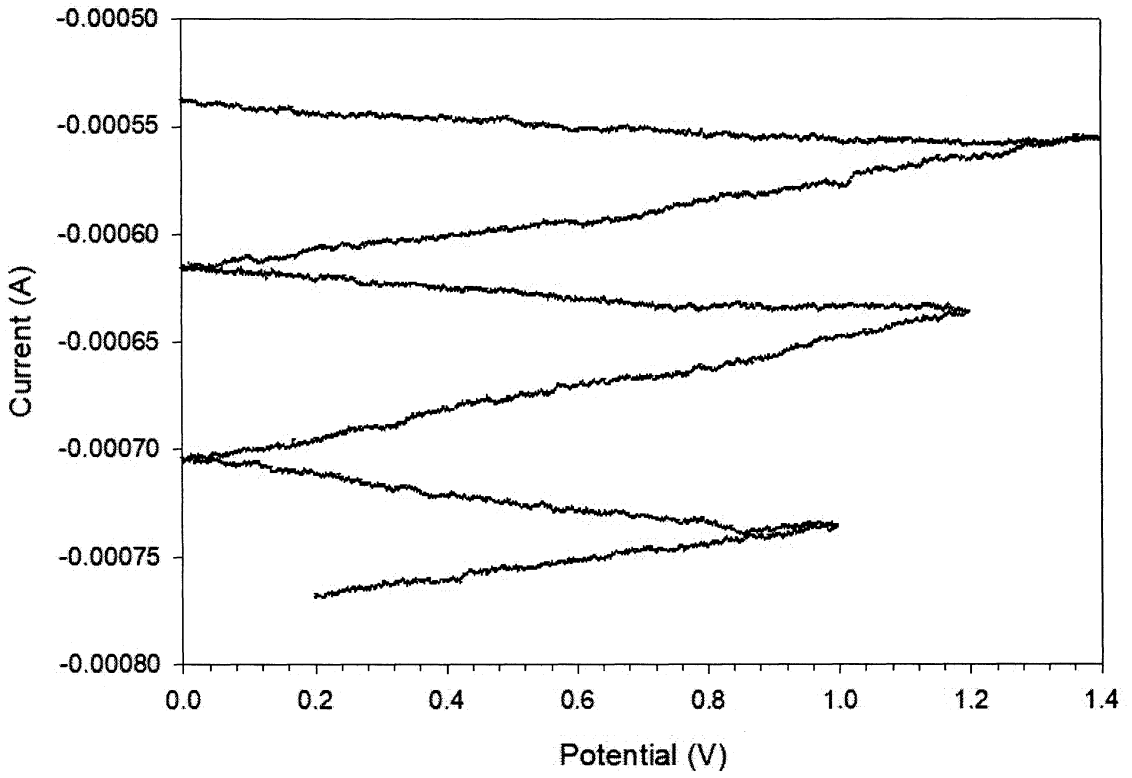

Figure 37. Sweep step scan on a 10 mm × 10 mm $SrTiO_3$ substrate (sample # 141103) with one contact, and the potential range was from 0 V to 1.0 V, then increased the high final potential 0.2 V by every two segments up to 1.4 V (scan rate: 0.01 V/s; RE: Hg/HgO). The sensitivity was 10^{-1} A/V.

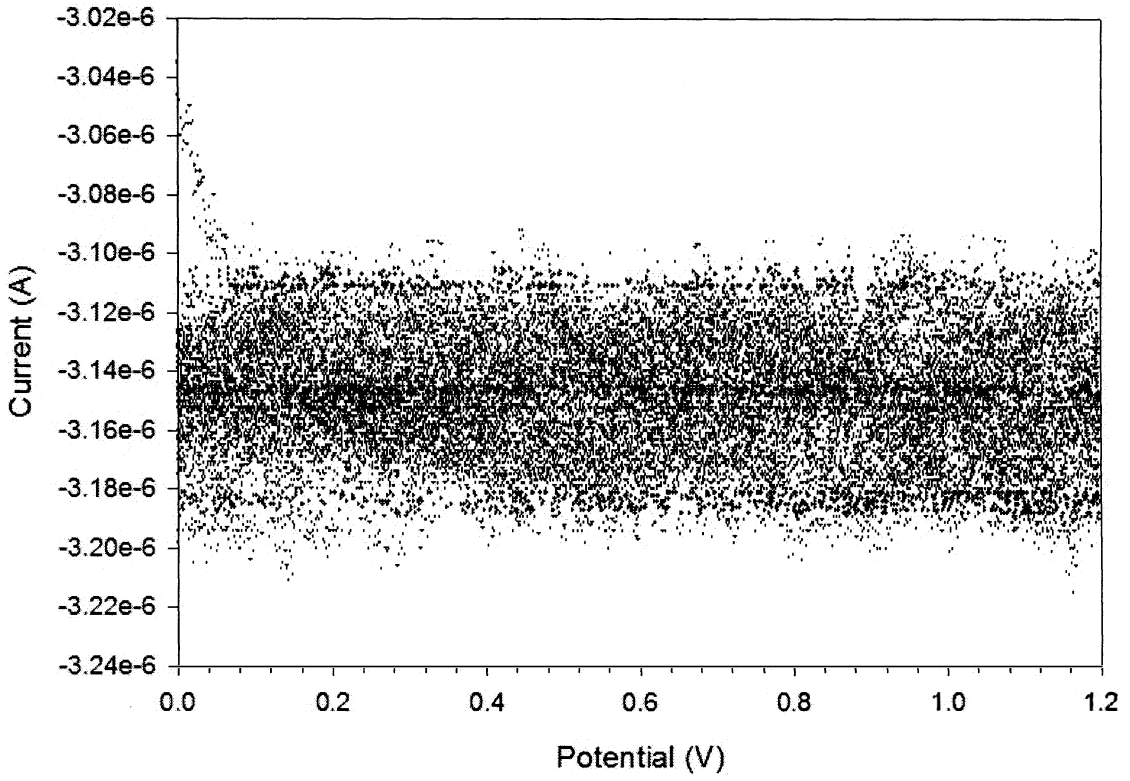

Figure 38. a) Cyclic voltammogram of background signal level testing on CHI-660C with the sensitivity level was setup as 1×10^{-3} A/V (scan rate: 0.1 V/s; RE: Hg/HgO). The sensitivity was 10^{-3} A/V. The order of magnitude of the current values is lesser than the sensitivity's by 3.

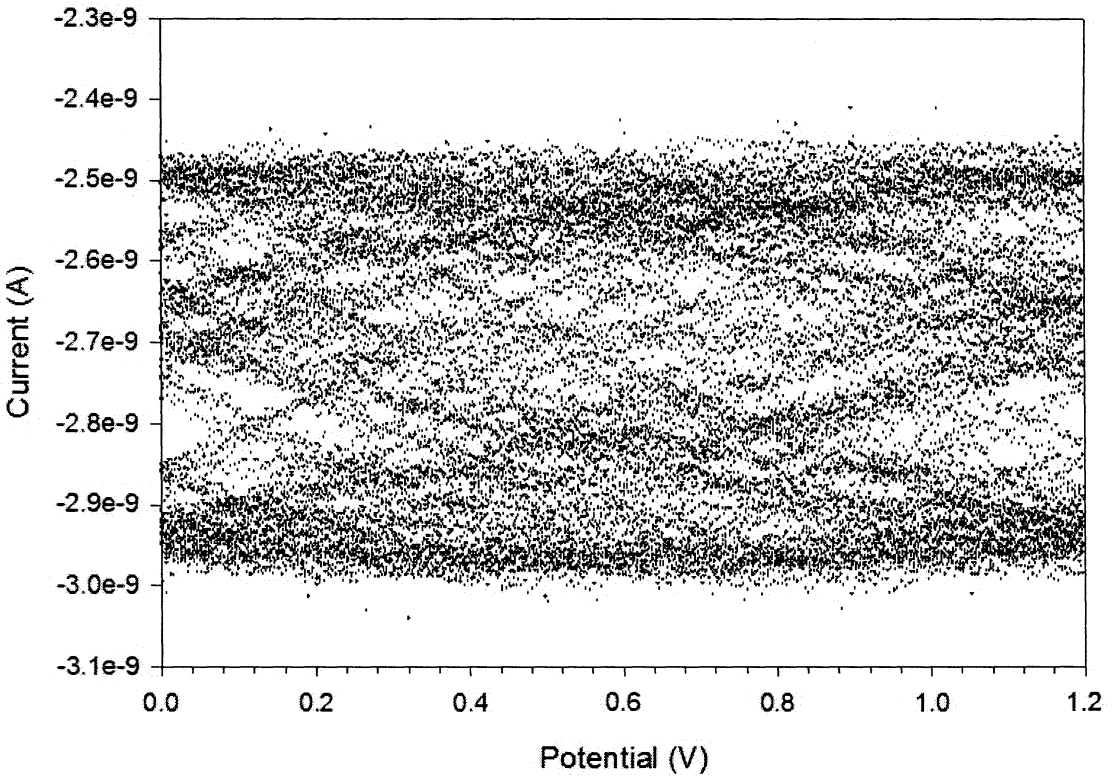

Figure 39. b) Cyclic voltammogram of background signal level testing on CHI-660C with the sensitivity level was setup as 1×10^{-6} A/V (scan rate: 0.1 V/s; RE: Hg/HgO). The order of magnitude of the current values is lesser than the sensitivity's by 3.

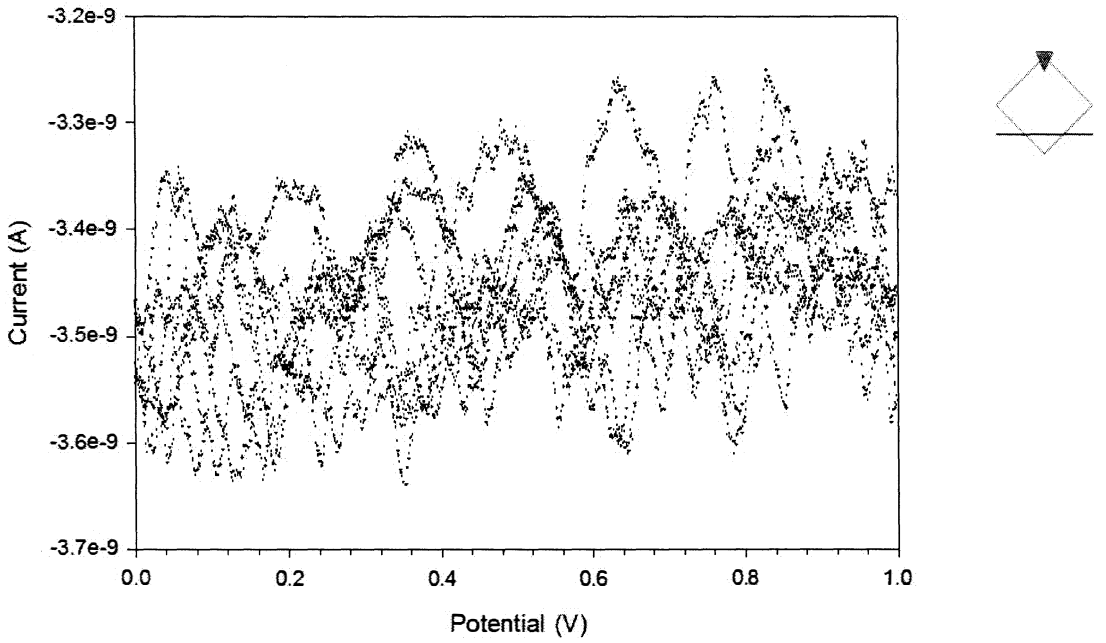

Figure 40. Cyclic voltammogram of a 10 mm × 10 mm $SrTiO_3$ substrate (sample # 150816) with least submerging level shown as right (scan rate: 0.05 V/s; RE: Hg/HgO). The sensitivity was 10^{-6} A/V.

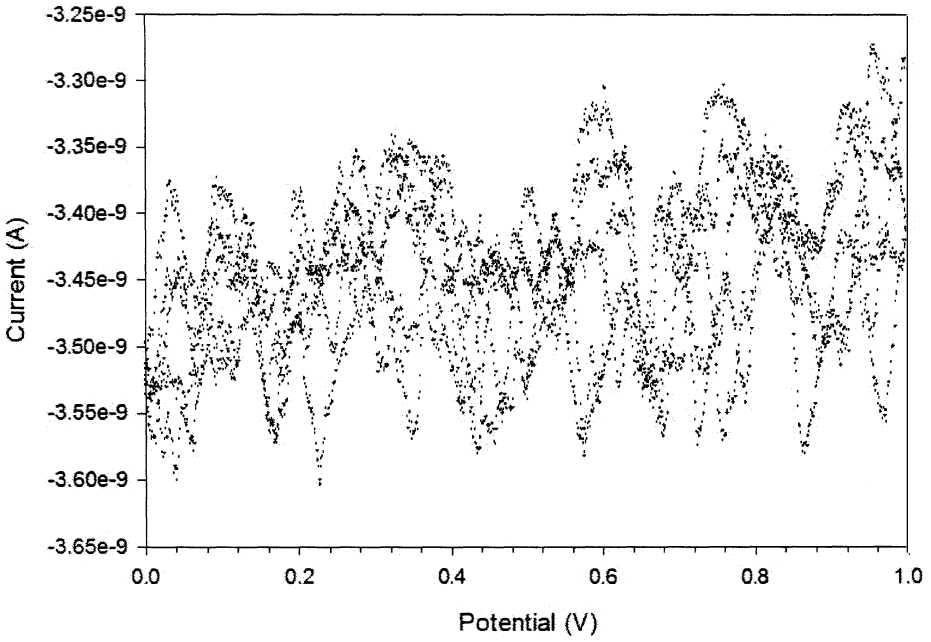

Figure 41. Cyclic voltammogram of a 10 mm × 10 mm $SrTiO_3$ substrate (sample # 150816) with near-half submerging level shown as right (scan rate: 0.05 V/s; RE: Hg/HgO). The sensitivity was 10^{-6} A/V.

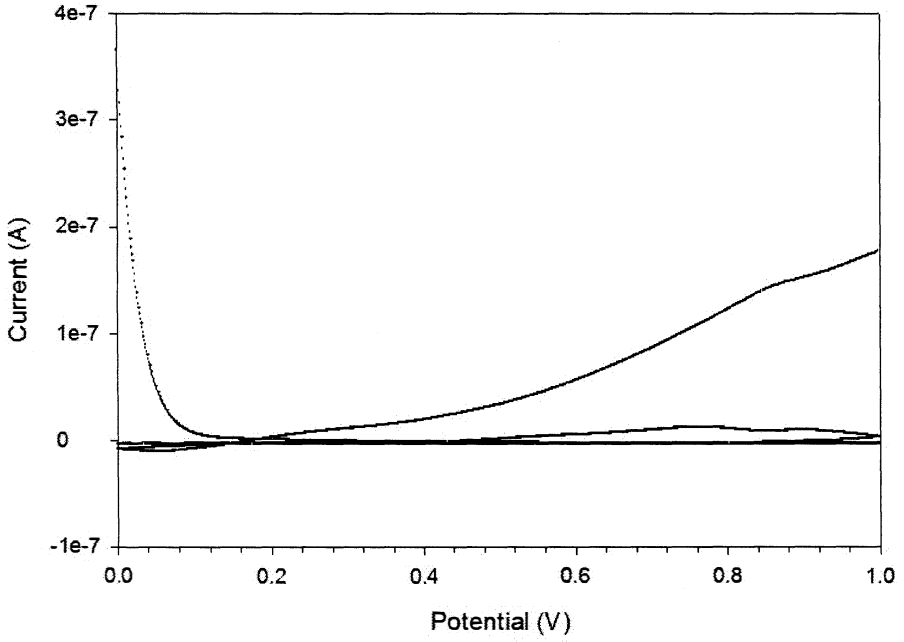

Figure 42. Cyclic voltammogram of a 10 mm × 10 mm $SrTiO_3$ substrate (sample # 150816) with over-half submerging level shown as right (scan rate: 0.05 V/s; RE: Hg/HgO). The sensitivity was 10^{-6} A/V.

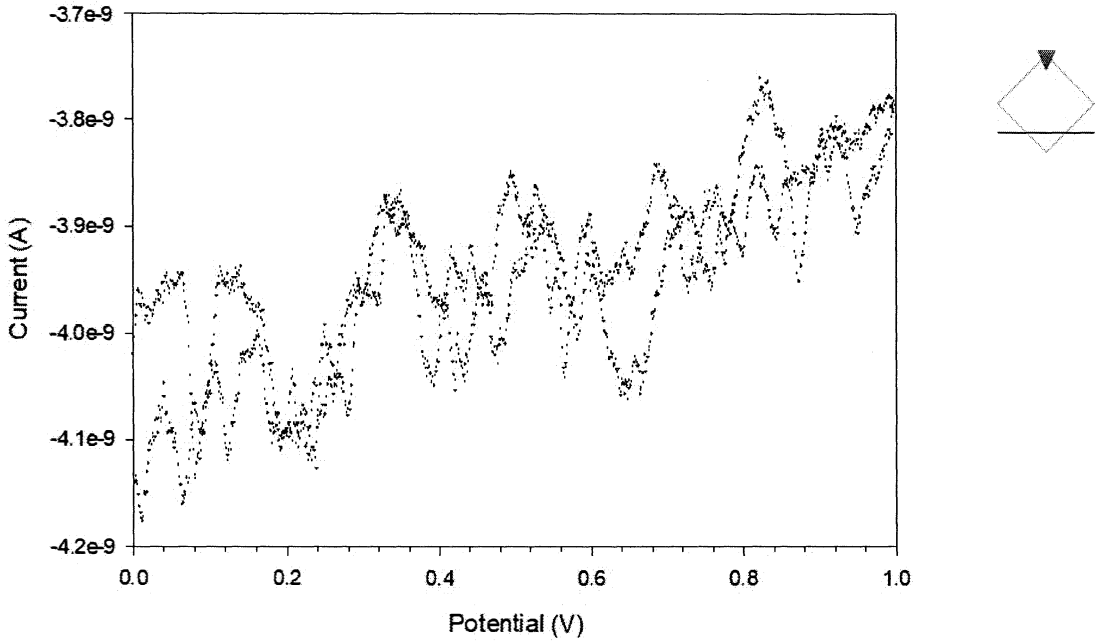

Figure 43. Cyclic voltammogram of a 10 mm × 10 mm $SrTiO_3$ substrate (sample # 150816) with least submerging level shown as right in 0.5 M NaOH (scan rate: 0.05 V/s; RE: Hg/HgO). The sensitivity was 10^{-6} A/V.

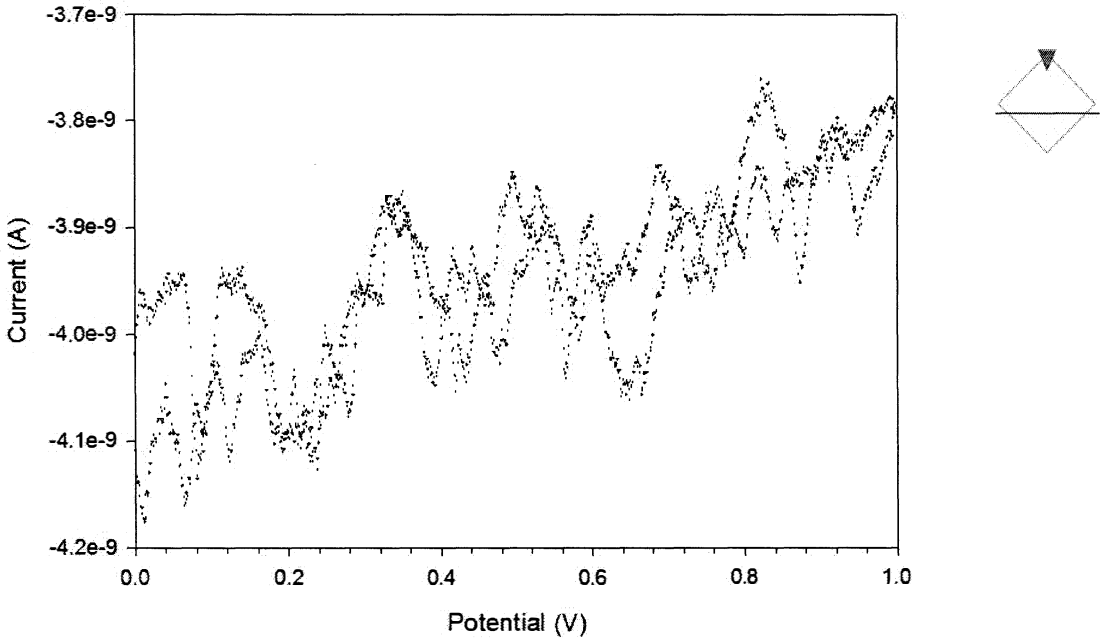

Figure 44. Cyclic voltammogram of a 10 mm × 10 mm $SrTiO_3$ substrate (sample # 150816) with near-half submerging level shown as right in 0.5 M NaOH (scan rate: 0.05 V/s; RE: Hg/HgO). The sensitivity was 10^{-6} A/V.

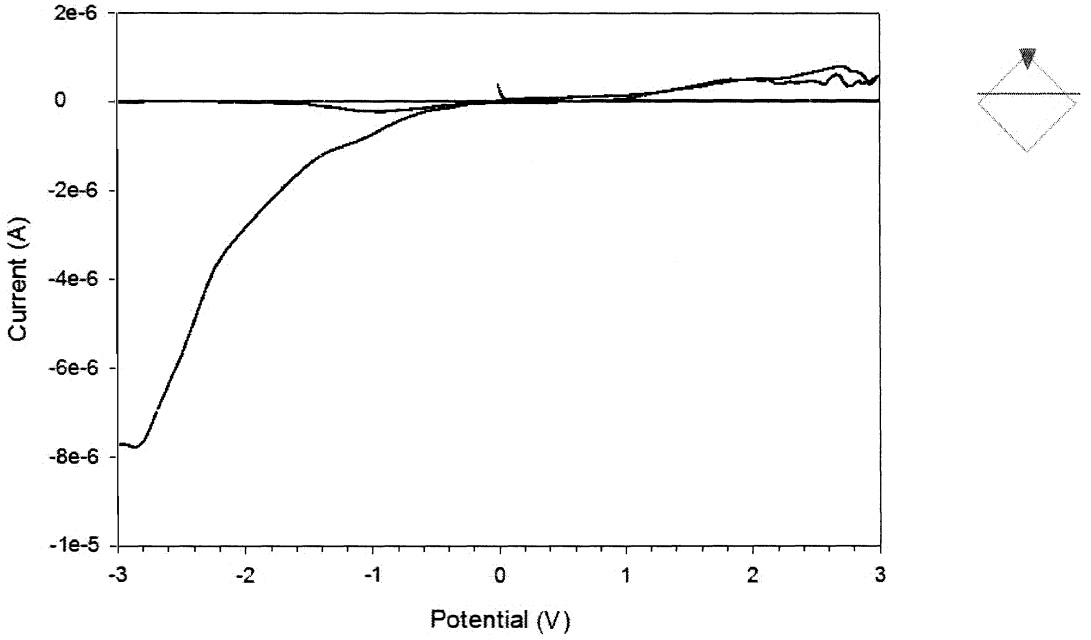

Figure 45. Cyclic voltammogram of a 10 mm × 10 mm $SrTiO_3$ substrate (sample # 150816) with over-half submerging level shown as right in 0.5 M NaOH (scan rate: 0.05 V/s; RE: Hg/HgO). The sensitivity was 10^{-6} A/V.

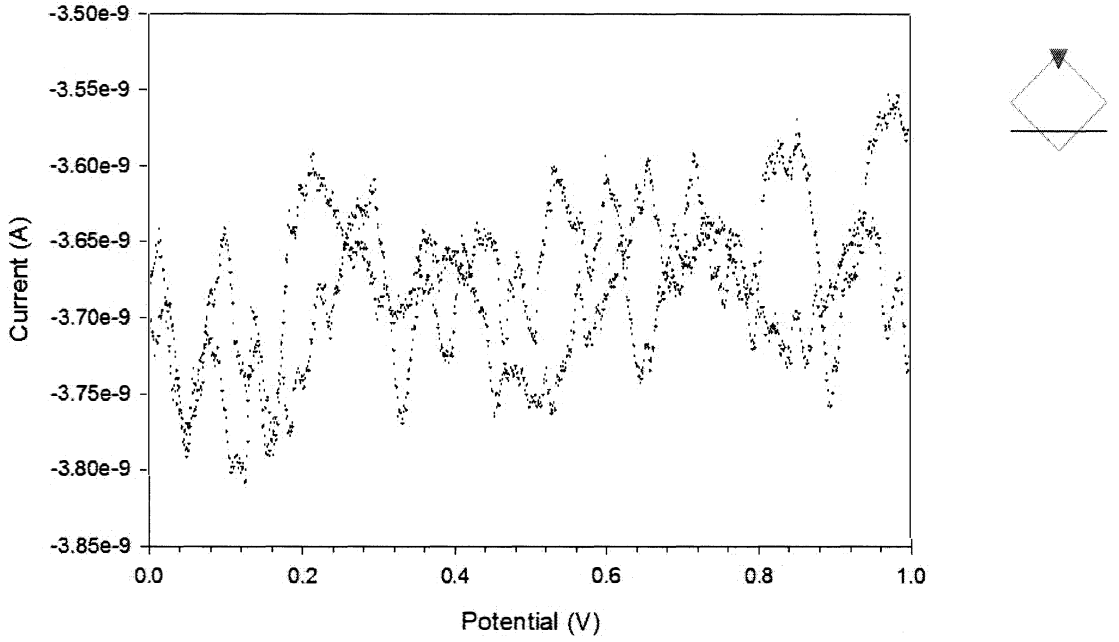

Figure 46. Cyclic voltammogram of a 10 mm × 10 mm $SrTiO_3$ substrate (sample # 150816) with least submerging level shown as right in 2 M NaOH (scan rate: 0.05 V/s; RE: Hg/HgO). The sensitivity was 10^{-6} A/V.

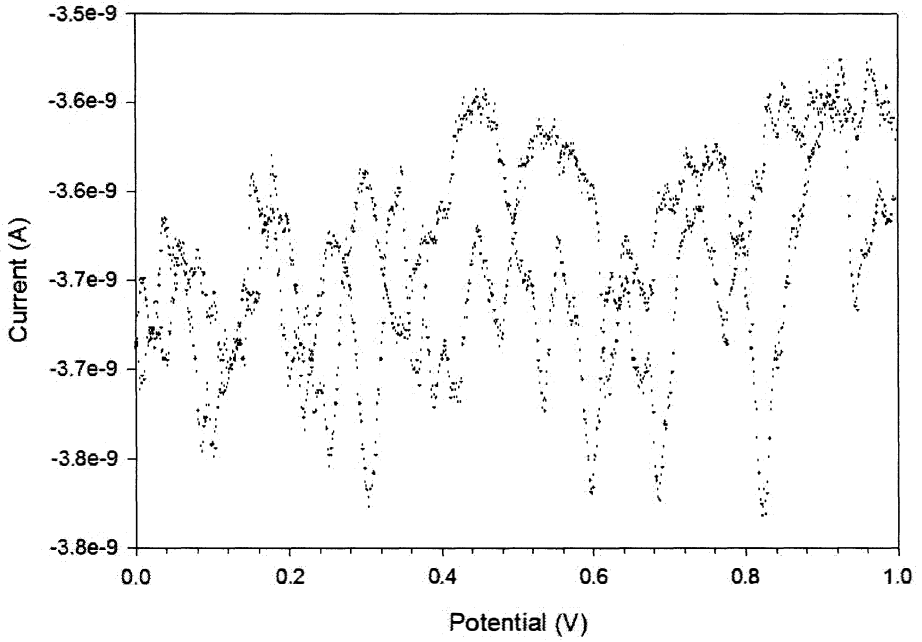

Figure 47. Cyclic voltammogram of a 10 mm × 10 mm $SrTiO_3$ substrate (sample # 150816) with near-half submerging level shown as right in 2 M NaOH (scan rate: 0.05 V/s; RE: Hg/HgO). The sensitivity was 10^{-6} A/V.

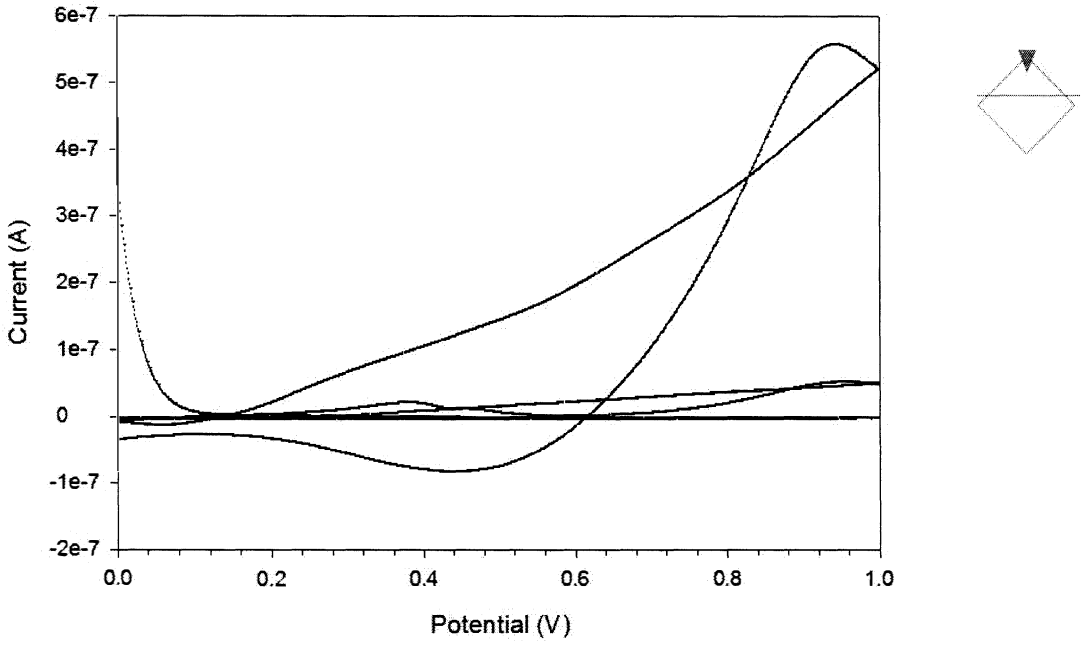

Figure 48. Cyclic voltammogram of on a 10 mm × 10 mm $SrTiO_3$ substrate (sample # 150816) with over-half submerging level shown as right in 2 M NaOH (scan rate: 0.05 V/s; RE: Hg/HgO). The sensitivity was 10^{-6} A/V.

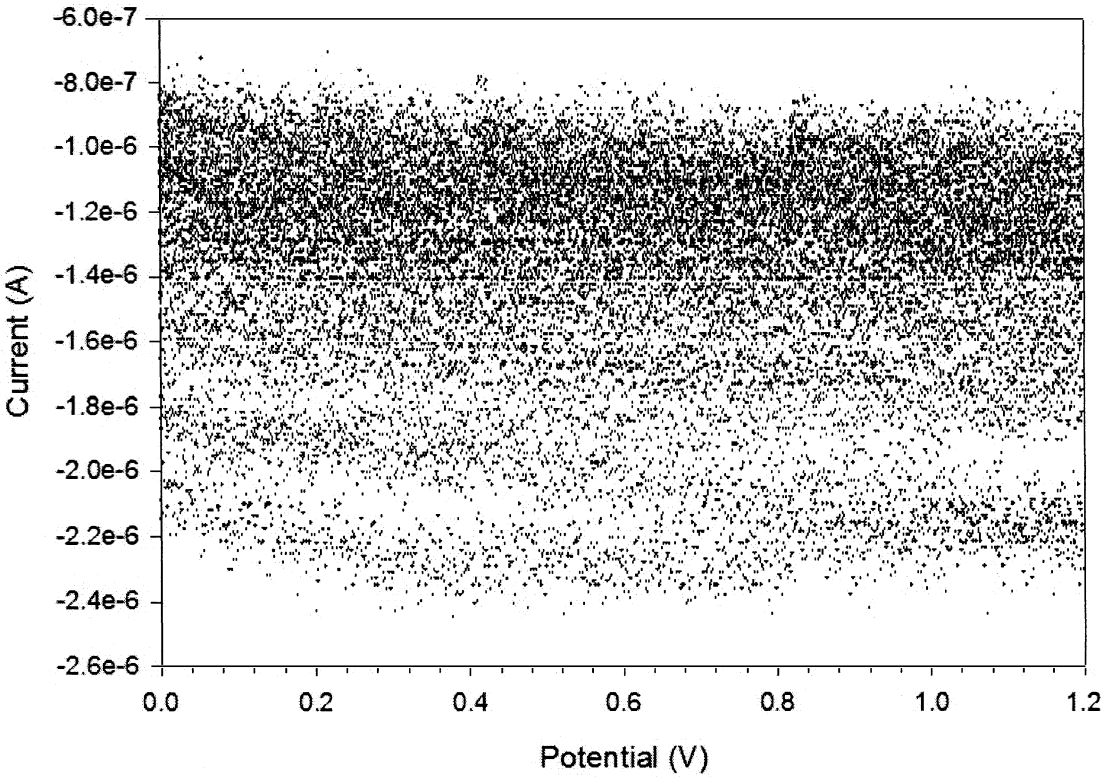

Figure 49. Cyclic voltammogram of background signal level testing on CHI-731E with the sensitivity level was setup as 1×10^{-3} A/V (scan rate: 0.1 V/s; RE: Hg/HgO). The order of magnitude of the current values is lesser than the sensitivity's by 3.

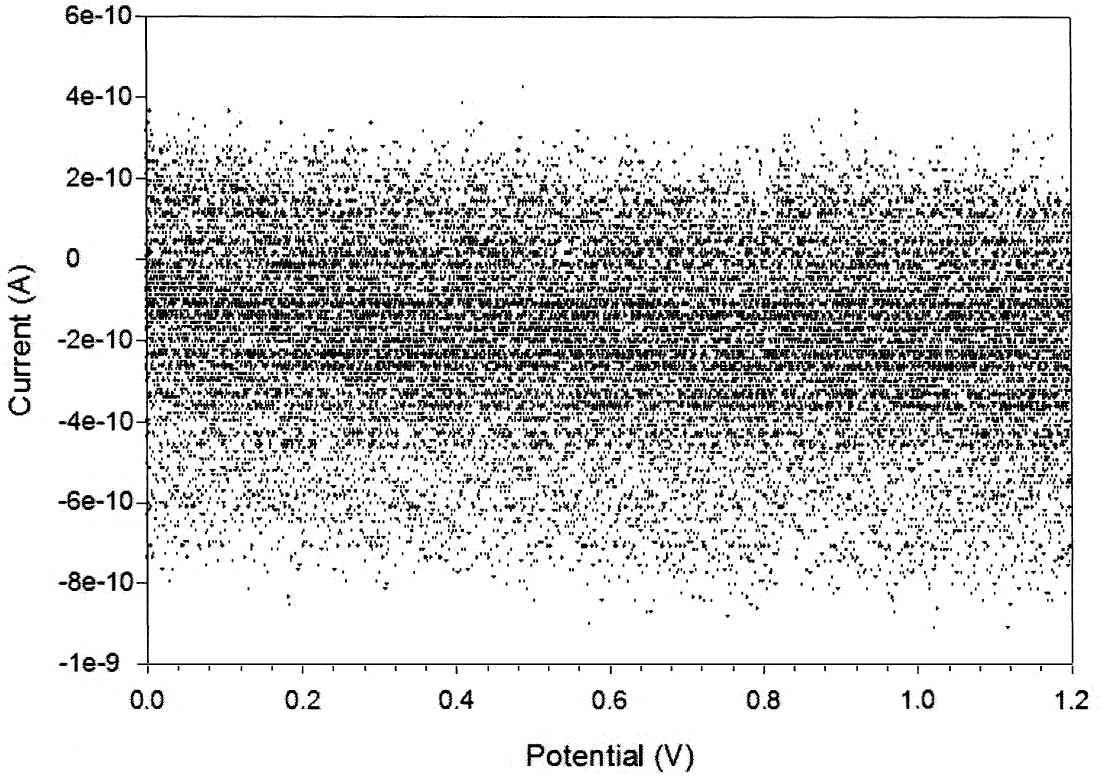

Figure 50. Cyclic voltammogram of background signal level testing on CHI-731E with the sensitivity level was setup as 1×10^{-6} A/V (scan rate: 0.1 V/s; RE: Hg/HgO). The order of magnitude of the current values is lesser than the sensitivity's by 4.

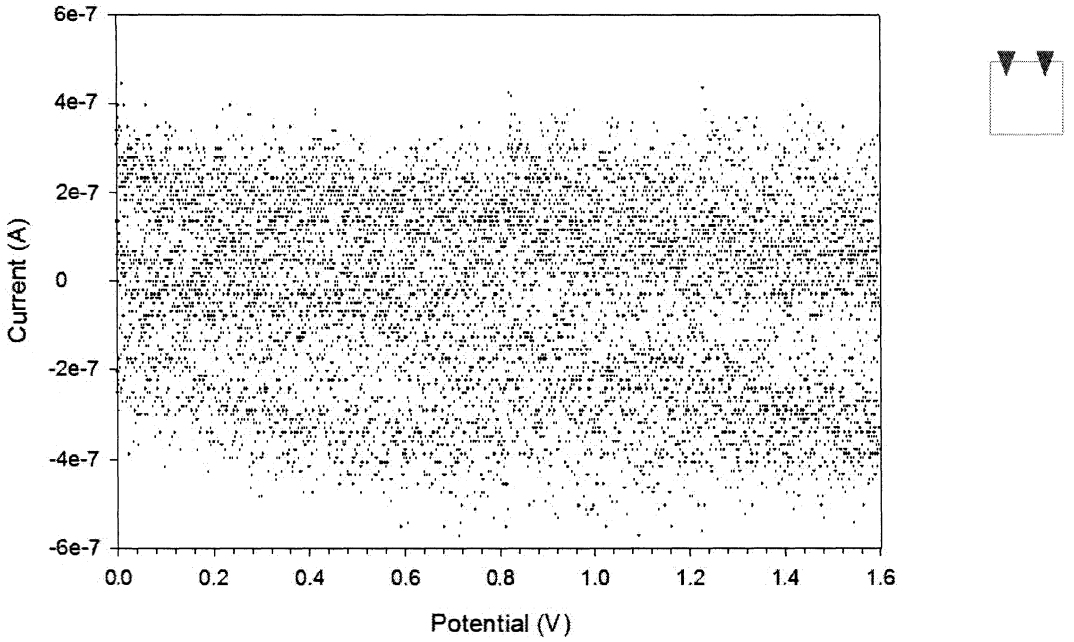

Figure 51. Cyclic voltammogram of a 10 mm × 10 mm $SrTiO_3$ substrate (sample # 20160419) with two contacts and least submerging level shown as right on CHI-731 potentiostats (scan rate: 0.1 V/s; RE: Hg/HgO). The sensitivity was 10^{-2} A/V.

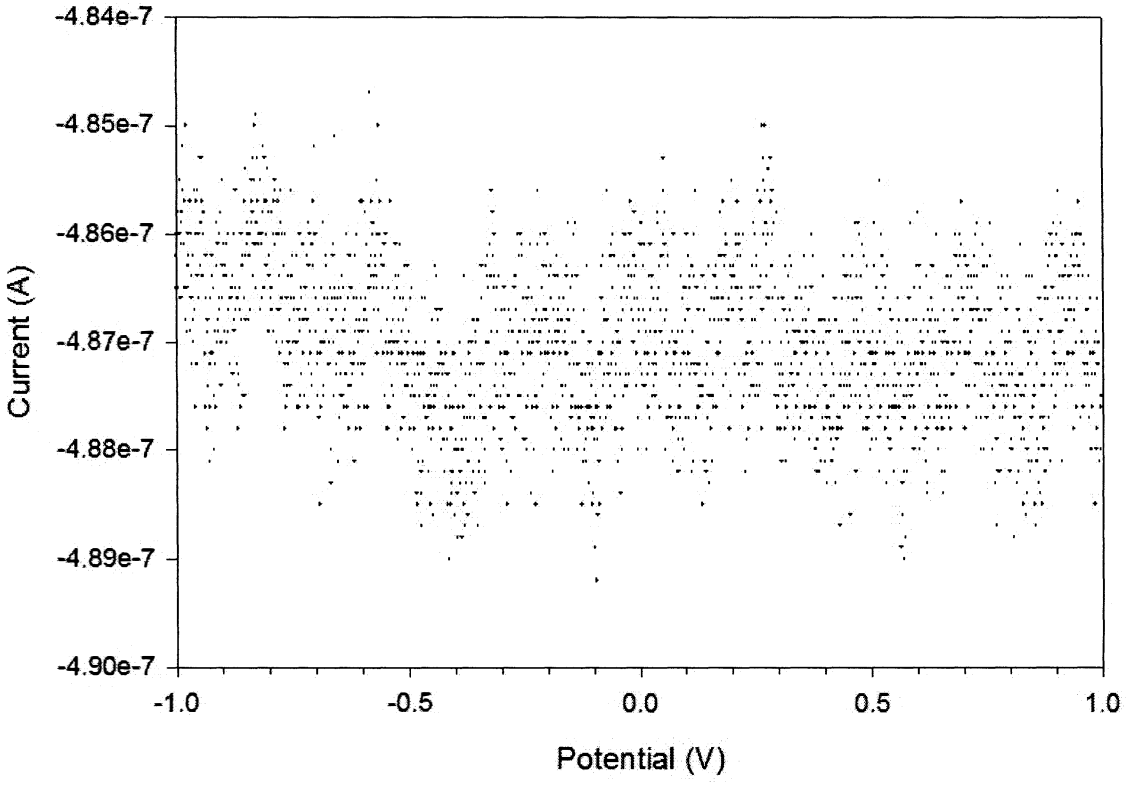

Figure 52. Cyclic voltammogram of a 5 mm × 5 mm $SrTiO_3$ substrate (1 contact; substrate was not immersed in electrolyte; scan rate: 0.1 V/s; RE: Hg/HgO). The sensitivity was 10^{-4} A/V.

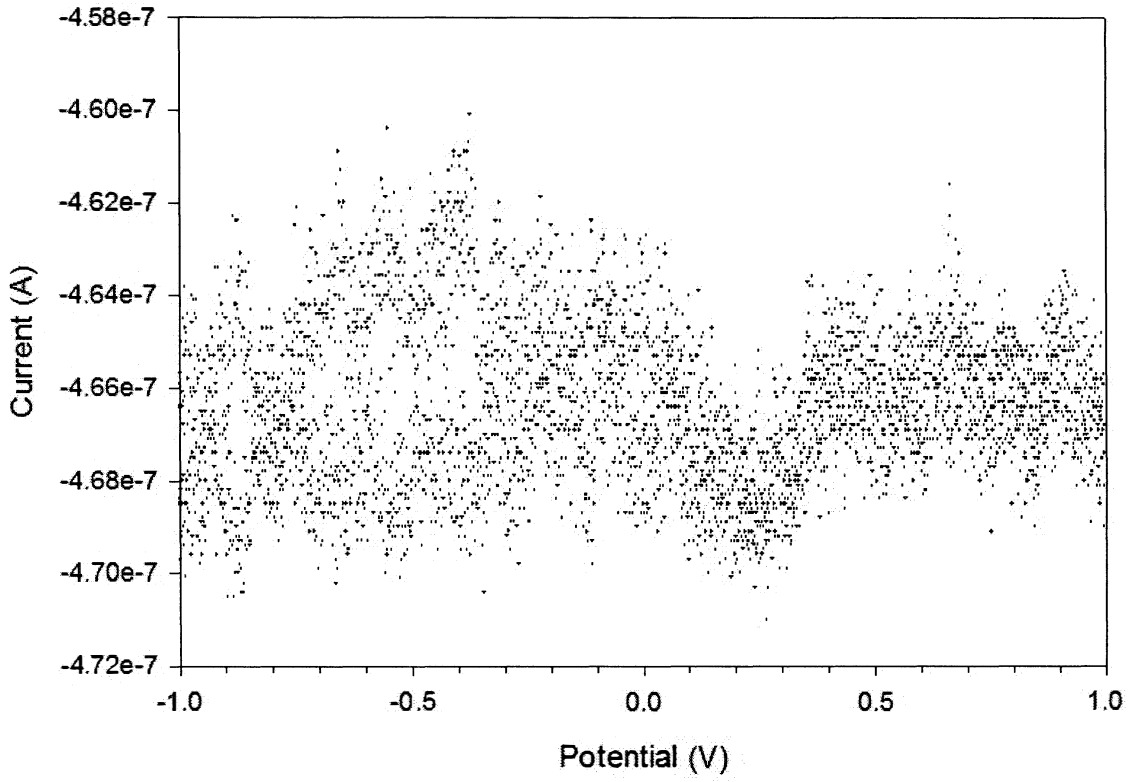

Figure 53. Cyclic voltammogram of a 10 mm × 10 mm $SrTiO_3$ substrate (1 contact; substrate was not immersed in electrolyte; scan rate: 0.1 V/s; RE: Hg/HgO). The sensitivity was 10^{-4} A/V.

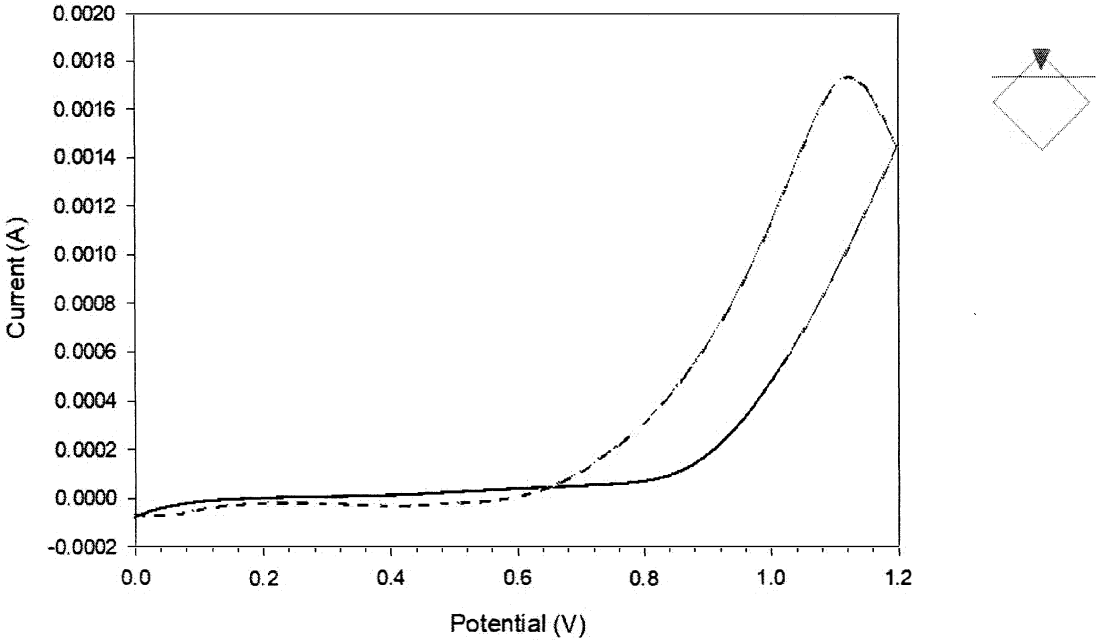

Figure 54. Cyclic voltammogram of a 5 mm × 5 mm $SrTiO_3$ substrate (sample # 20160126) excessively submerged (immersion depth shown as right, scan rate: 0.05 V/s; RE: Hg/HgO). The sensitivity was 10^{-3} A/V.

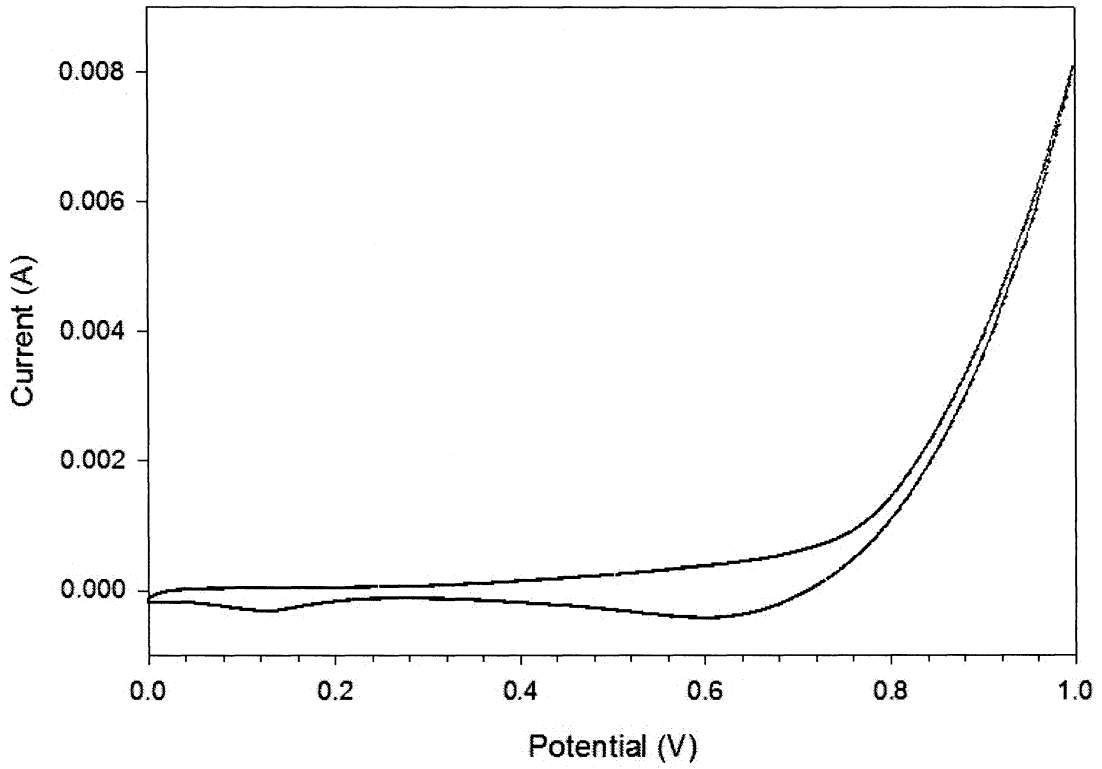

Figure 55. Cyclic voltammogram of a gold coated clamp (no $SrTiO_3$ substrate clipped; scan rate: 0.1 V/s; RE: Hg/HgO). The sensitivity was 10^{-3} A/V.

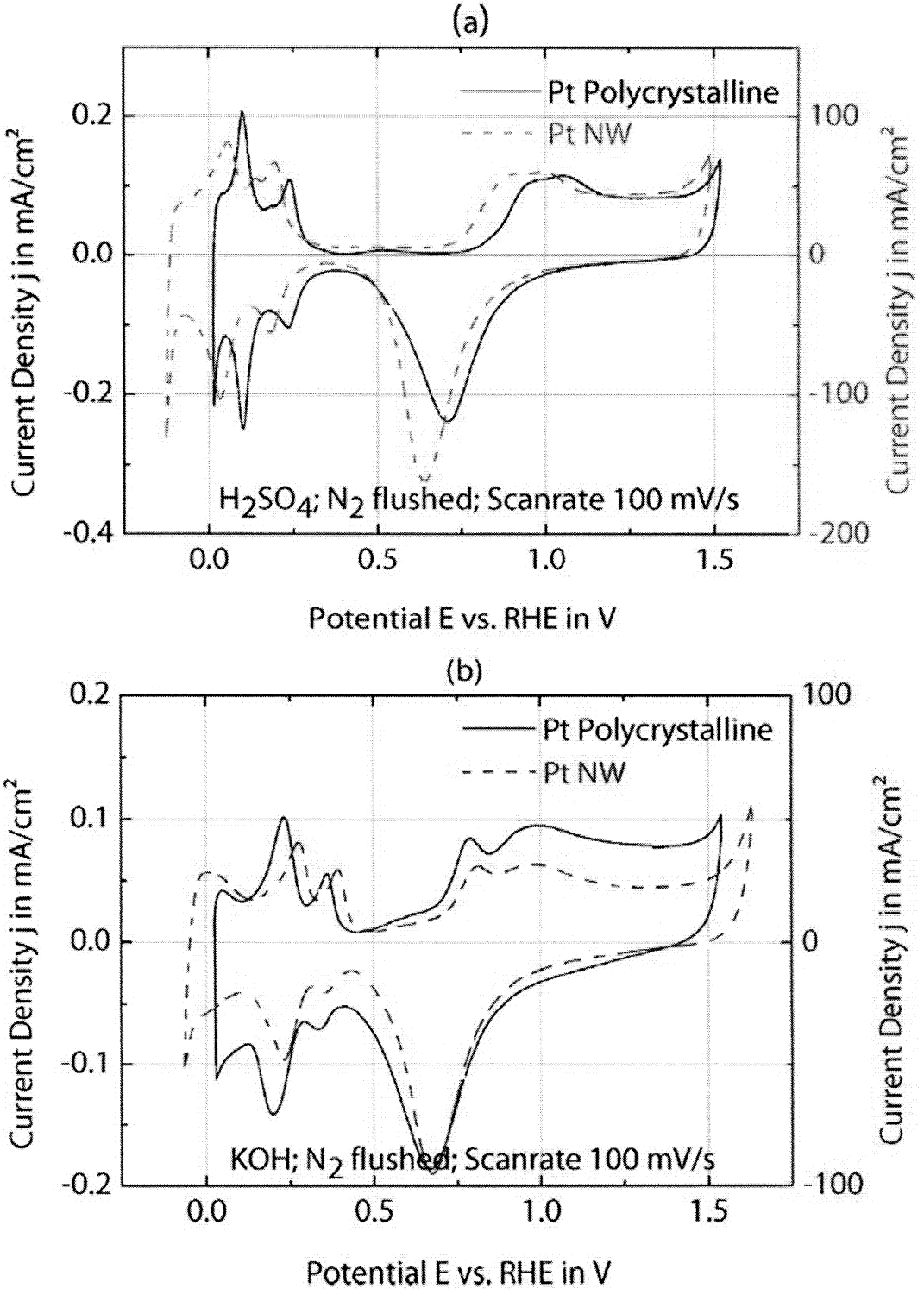

Figure 56. Reference cyclic voltammogram of Pt polycrystalline (solid) in both H_2SO_4 (a) and KOH (b) solution (from reference 25).